NBSIR 75-754

NASA CR-134869

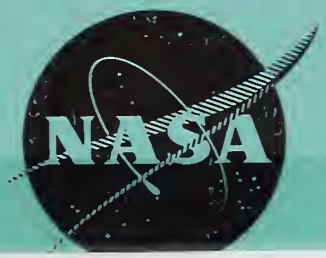

ALKALI OXIDE-TANTALUM, NIOBIUM AND ANTIMONY OXIDE IONIC CONDUCTORS

by

R. S. Roth, W. S. Brower, H. S. Parker, D. B. Minor and J. L. Waring

prepared for

NATIONAL AERONAUTICS AND SPACE ADMINISTRATION

CONTRACT C-50821-C

U.S. DEPARTMENT OF COMMERCE
NATIONAL BUREAU OF STANDARDS
WASHINGTON, D. C. 20234

TABLE OF CONTENTS

SUMMARY 3

1.0 INTRODUCTION 5

2.0 DISCUSSION OF RESULTS 6

2.1 The System Nb_2O_5-$4Rb_2O$:$11Nb_2O_5$ 6

2.2 The System Ta_2O_5-$4Rb_2O$:$11Ta_2O_5$ 6

2.3 The System Sb_2O_4-$NaSbO_3$ 7

2.3.1 $NaSbO_3$ 8

2.3.2 Pyrochlore Solid Solution 8

2.3.3 Polymorphism of Sb_2O_4 10

2.4 The System Sb_2O_4-$KSbO_3$ 11

2.4.1 Hydroxyl Ion Stabilization of Cubic Potassium Antimonate 11

2.5 The System Sb_2O_4-$NaSbO_3$-NaF 13

2.5.1 The System $NaSbO_3$-NaF 13

2.5.2 The Ternary System 14

2.6 Other Systems 15

2.6.1 Alkali Bismuthates 15

2.6.2 Alkali-Rare Earth Systems 15

2.6.3 Further Studies in the System Nb_2O_5:$KNbO_3$ 16

2.7 Pellet Fabrication 16

2.7.1 $41K_2O$:$59Nb_2O_5$ ("2:3", $K_4Nb_6O_{17}$) 16

2.7.2 $4Rb_2O$:$11Nb_2O_5$ (11-layer phase) 18

2.7.3 Large Pellets for Ionic Conductivity Measurements 18

2.8 Crystal Growth and Synthesis 20

2.8.1 Crystal Growth by Pulling from the Melt 20

2.8.1.1 Hexagonal Tungsten Bronze in the K_2O-Ta_2O_5-WO_3 System 20

2.8.1.2 The System $KNbO_3$-Nb_2O_5 22

2.8.1.3 The System Rb_2O-Nb_2O_5 22

2.8.2 Flux Growth 23
2.8.2.1 The System Rb_2O-Nb_2O_5-MoO_3 23
2.8.2.2 The System Rb_2O-Ta_2O_5-MoO_3 24
2.8.2.3 The System Rb_2O-Ta_2O_5-RbF 24
2.8.2.4 The Systems $ASbO_3$-Sb_2O_4-AF (A = Na,K.Rb) 24
2.9 Ion Exchange 26
3.0 RELATION OF STRUCTURAL MECHANISMS OF NON-STOICHIOMETRY TO IONIC CONDUCTIVITY 27
3.1 Hexagonal Tungsten Bronze-type Phases (HTB) 28
3.2 Pyrochlore Phases 28
3.3 Hexagonal Tungsten Bronze - Pyrochlore Series 31
3.4 Body Centered Cubic Antimonates 32
3.5 The Phase $2K_2O:3Nb_2O_5$ 35
4.0 SUMMARY OF RESULTS 36
5.0 FUTURE WORK 37
REFERENCES 38
FIGURE CAPTIONS 40
TABLES OF EXPERIMENTAL DATA 50
DISTRIBUTION LIST 69

SUMMARY

This report summarizes work carried out between January 1, 1974 and December 31, 1974 under an agreement with the National Aeronautics and Space Administration, Lewis Research Center (Interagency Agreement PR545160) to study the phase equilibria of alkali oxide-tantalum, niobium and antimony oxide systems and synthesis of phases which might have interesting ionic conductivity. It also includes work performed since the last contract (Interagency Order C-29933-C [1]) which ended in October 1973, as well as that done since the formal ending of the present contract and the issuance of this summary report.

In addition to the six systems reported in the previous contract (Interagency Order C-29933-C [1]) the phase equilibrium relations of four additional systems were investigated in detail. These consisted of sodium and potassium antimonates with antimony oxide and tantalum and niobium oxide with rubidium oxide as far as the ratio $4Rb_2O:11B_2O_5$ (B=Nb, Ta). The ternary system $NaSbO_3$-Sb_2O_4-NaF was also investigated extensively to determine the actual composition of the body centered cubic sodium antimonate. In addition, various other binary and ternary oxide systems involving alkali oxides were examined in lesser detail. The phases synthesized were screened by ion exchange methods to determine mobility of the alkali ion within the niobium, tantalum or antimony oxide (fluoride) structural framework.

Five structure types were found to be of sufficient interest to warrant further investigation. These structure types are (1) hexagonal tungsten bronze (HTB) (2) pyrochlore (3) the hybrid HTB-pyrochlore hexagonal ordered phases (4) body centered cubic antimonates and (5) $2K_2O:3Nb_2O_5$. Although all of these phases exhibit good ion exchange properties only the pyrochlore in the Sb_2O_4-$NaSbO_3$ system has so far been prepared with Na^+ ions as an equilibrium phase and as a low porosity

ceramic. Unfortunately Sb^{+3} in the channel apparently interferes with ionic conductivity in this case, although relatively good ionic conductivity was found for the metastable Na^{+} ion exchanged analogs of $RbTa_2O_5F$ and $KTaWO_6$ pyrochlore phases. Small crystals of the other phases can generally be prepared by flux techniques and ion exchanged with Na^{+}. However, in the one case where congruency allows large crystals to be pulled from the melt ($4Rb_2O:11Nb_2O_5$) ion exchange techniques up to ~450°C are not sufficient to accomplish replacement with Na^{+} ions.

1.0 INTRODUCTION

The program described in the present report involves the preparation of single crystals and ceramic specimens of materials which have passed some preliminary screening tests and appear to be potential candidates as solid ionic conductors. Much of the preliminary screening was done under previous work order (No. C-29933-C) [1]. Furthermore the phase equilibrium diagrams have been studied for some systems in which promising candidates have been discovered but for which no phase data existed.

Crystals and ceramic specimens were prepared or synthesis attempted for various different structure types and compositions, including the hexagonal tungsten bronze and pyrochlore phases in the system K_2O-Ta_2O_5-WO_3, the $2K_2O$:$3Nb_2O_5$ type phase and the phases in the system Rb_2O-Nb_2O_5. In addition specimens of the pyrochlore phase and the body centered cubic phase of the $NaSbO_3$-Sb_2O_4-NaF system were examined.

The phase equilibria diagrams of the Rb_2O-Nb_2O_5 and Rb_2O-Ta_2O_5 systems were examined as well as those of the Sb_2O_4-$NaSbO_3$ and Sb_2O_4-$KSbO_3$. In addition the equilibria in the system Sb_2O_4-$NaSbO_3$-NaF were investigated. Other compositions examined included the alkali rare earth oxide systems and alkali oxide-bismuth oxide systems although no high temperature equilibrium phases were found in any of these systems.

The method of flux synthesis was used to prepare small single crystals for the first time of the pyrochlore phase $RbTa_2O_5F$ and the body centered cubic phases of F^- stabilized potassium and sodium antimonates.

In the following discussion all ratios (1:3, 3:5, etc.) refer to the alkali/metal ratio rather than to the particular starting material that may have been used.

2.0 DISCUSSION OF RESULTS

2.1 The System Nb_2O_5-$4Rb_2O$:$11Nb_2O_5$

The system Rb_2O-Nb_2O_5 was investigated from the region of about 27 mole % Rb_2O to the Nb_2O_5 end member. Ten compositions were prepared by dry mixing stoichiometric amounts of Rb_2CO_3 and Nb_2O_5 and calcining in open Pt crucibles at 500°C and 600°C for extended periods of time with intermediate grindings. The specimens were heated at higher temperatures in sealed Pt tubes in resistance wound quench-type furnaces (Table 1). The x-ray diffraction patterns of these quenched specimens were used to establish the phase equilibrium diagram shown in Figure 1.

Single crystals of the eleven layer (11-L) ($4Rb_2O$:$11Nb_2O_5$), hexagonal tungsten bronze (HTB) ($21.75Rb_2O$:$78.25Nb_2O_5$) and Gatehouse tungsten bronze (GTB) ($11.5Rb_2O$:$88.5Nb_2O_5$) phases (see reference [1] for nomenclature of phases) were grown from the melt by modified Czochralski techniques. Single crystal fragments of the 11-L phase were used in ion exchange experiments but did not provide better results than isostatically pressed pellets prepared from calcined powder.

Unit cell dimensions for all phases are given in the summary table of x-ray data at the end of this report (Table 12). They were determined from both single crystal precession patterns and x-ray powder diffraction patterns (CuKα radiation, Ni filtered) with the aid of a computer least squares program. Only the phase occurring at low temperatures at about 15 mole % Rb_2O has not been indexed, as no single crystals were obtained.

2.2 The System Ta_2O_5-$4Rb_2O$:$11Ta_2O_5$

The system Rb_2O-Ta_2O_5 was investigated from 26.67 mole % Rb_2O to 100 mole % Ta_2O_5. Eight compositions were prepared and the system was investigated by conventional quenching methods. The samples were heated in open Pt trays at 500° and 600°C and then heated in sealed

Pt tubes at higher temperatures. The phases were identified by comparison with known structures in the K_2O-Ta_2O_5 and Rb_2O-Nb_2O_5 systems. Equilibria was assumed to have been established when successive heat treatments showed no change in the x-ray diffraction patterns. As in the K_2O-Ta_2O_5 [1,2] and Rb_2O-Nb_2O_5 systems a layer sequence 9-L, 16-L, 11-L (in order of increasing alkali content) was found to be present. The HTB and GTB-like phases [1] were also found to be present. The results of the experiments are given in Table 2 and the phase equilibrium diagram interpreted from this data is shown in Figure 2.

2.3 The System Sb_2O_4-$NaSbO_3$

The system between the compositional limits of $NaSbO_3$ and Sb_2O_4 has been examined in detail. Thirteen compositions were studied by air by conventional quenching techniques and the materials were examined by single crystal, powder, and high temperature x-ray diffraction techniques. The phase equilibrium diagram, Figure 3, has been constructed from the data given in Table 3. When Sb_2O_4 is reacted at low temperature (~750-1000°C) with alkali carbonate it generally looses the CO_2 and picks up oxygen from the atmosphere to satisfy equilibrium conditions of the phases formed, which may involve oxidation of the antimony ions. Therefore the antimonate systems reported here are not strictly binary.

The compound $NaSbO_3$ (ilmenite-type) was found in this work to melt at about 1555±5°C. An intermediate pyrochlore solid solution exists from about 37.5 mole % Na_2O:62.5 mole % Sb_2O_4 to 24 mole % Na_2O:76 mole % Sb_2O_4 at 1350°C. The 1:3 composition probably does not really correspond structurally to $[NaSb^{+3}]Sb_2^{+5}O_7$ although the 3:5 composition may be written as $[Na_{1.5}Sb^{+3}_{.5}]Sb_2^{+5}O_{6.5}$ see Section 3.2. The $3Na_2O$:$5Sb_2O_4$ composition apparently melts congruently at 1490±5°C. The solidus curve falls from this temperature to about 1340±5°C at 24 mole % Na_2O:76 mole % Sb_2O_4. A two phase region exists between the pyrochlore solid solution and Sb_2O_4. An unknown phase was found to occur in the system which could

be made approximately single phase by calcining the composition 15 mole % Na_2O:85 mole % Sb_2O_4 at 750°C and reheating in a sealed Pt tube to 1000°C for 64 hours in the presence of PtO_2. This phase has an as yet unindexed x-ray diffraction pattern with the four strongest lines occurring at d values equal to 3.283, 2.798, 3.453, 8.23A.[1/]

2.3.1 $NaSbO_3$

The compound Na_2O:Sb_2O_5 was first reported to occur by Schrewelius [4] and to be hexagonal with a=5.316 and c=15.95A and an ilmenite structure. This compound was found in the present work to melt congruently at about 1555±5°C. No other stable polymorphs were encountered.

2.3.2 Pyrochlore Solid Solution

One intermediate phase, a cubic pyrochlore solid solution mentioned by Stewart and Knop [5], was characterized in the system. The compositional varies from approximately Na_2O:$3Sb_2O_4$ to $3Na_2O$:$5Sb_2O_4$ with unit cell dimensions varying from 10.289 to 10.286A respectively. Since the pyrochlore is a tunnel structure and since this pyrochlore is the only one reported that contains sodium that can be formulated by direct synthesis it was worthy of further study as a possible ionic conductor. For ionic conductivity measurements dense materials were needed and several experiments were conducted with Na_2O:Sb_2O_4 (1:2) in an effort to determine its stability under high pressure and temperature. In the first experiment, 2.25 g of single phase pyrochlore material were prepressed at 10,000 psi,[2/] packed into a Pt cylinder 3/8 O.D. x 1 1/2" long with PtO_2 and sealed. This sealed crucible was heated to 1000°C and 69,800 psi with catastrophic results. Apparently this phase is not completely stable in this temperature-pressure range and some of the material reacted with the Pt container resulting in a melting of the Pt. The remaining

---

[1/] 10Å = 1.0 nanometers

[2/] The use of psi, bar, and kbar follows the current common practice of workers in the field. Note that 1 bar = 10^5 N/m^2 (or pascal) = 10^6 dyn/cm^2 = 0.9869 atm = 14.504 psi. The accepted international standard (SI) unit of pressure is the pascal or newton per meter squared.

specimen, slightly depleted in antimony oxide, was found by x-ray diffraction to contain a pyrochlore phase plus ilmenite (1:1).

The next experiment was scaled down in amount of material and pressure. A few milligrams of material were sealed in a 3 mm diameter Pt tube and heated to 700°C and 4,000 psi for 1 hour in the presence of PtO_2. The material remained 1:2 (pyrochlore) with slight sintering. A similar experiment was conducted at 1000°C and 4,000 psi for 2 hours. The PtO_2 was decomposed and there was grain growth. The x-ray pattern was of 1:2 pyrochlore. In the next experiment, two samples in sealed platinum tubes were heated at 1100°C and 5,000 psi for 3 hours. Platinum oxide was added to only one of the tubes before sealing. The specimen without PtO_2 was a single phase pyrochlore which appeared to be a very dense material. The measured density was 5.21 g/cm^3. The specimen containing PtO_2 was not dense.

In the last experiment two 5 mm diameter x 1 1/4" long tubes were flattened (to a rectangular shaped cross section, 1.5 mm thick) packed with material, sealed and heated to 1100°C and 4,000 psi. After heating, this specimen was very thin and brittle and the specimen fragmented when the Pt was mechanically removed. Again the specimen was quite hard with a measured density of 5.26 to 5.29 g/cm^3. The average density of four measured fragments was 5.26±.05 g/cm^3.

For ionic conductivity measurements, pellets of $Na_2O{:}2Sb_2O_4$ (3/4" in diameter) were placed in sealed platinum foil envelopes and hot pressed by a commercial company at 1100°C and 5,000 psi. The pellets were well formed single phase material with a density of 96% theoretical (See Section on Mechanisms of Non-stoichiometry 3.2). The ionic conductivity of these pellets was measured at NASA Lewis Research Center (LeRC) [6] and they were found to be essentially insulators.

The distribution of the various ions (i.e. Na^+, Sb^{+3}, Sb^{+5}, O^{-2}) in the $Na_2O{:}2Sb_2O_4$ has not as yet been determined from single crystal structure analysis. The structure of this material is currently

being determined at NBS. Until the results of this analysis are forthcoming it may be assumed that the "lone pair" electrons associated with Sb^{+3} will not allow the passage of Na^{+} through the channels.

2.3.3 Polymorphism of Sb_2O_4[3/]

Two stable polymorphs of Sb_2O_4 have been reported in the literature. They are α-Sb_2O_4 which is orthorhombic [7] a=5.436, b=11.76, c=4.810A and β-Sb_2O_4 which is monoclinic [8] a=11.905, b=4.834, c=5.383A and β=101°22'. From Table 4(a) it can readily be seen that specimens quenched from a temperature composition region represented on the phase diagram, Figure 3, as Sb_2O_4 + pyrochlore may contain either α-Sb_2O_4 and/or β-Sb_2O_4 when quenched from high temperatures and ambient pressures and examined at room temperature. From this seemingly inconsistent data it would appear that the α-Sb_2O_4 form and β-Sb_2O_4 form have a polytypic relationship. To help resolve this problem a high resolution electron microscope study should be done.

From the date in Table 4(b) it appears that the β form is the equilibrium high pressure form of Sb_2O_4. Insufficient data has been collected to establish if an equilibrium boundary curve exists between α-Sb_2O_4 and β-Sb_2O_4 at various temperatures and pressures. When specimens are sealed and heated under pressure in the presence of PtO_2 in either Pt or Au tubes single phase β-Sb_2O_4 is obtained. However when heated under pressure without the PtO_2, a two phase specimen results, β-Sb_2O_4 and the dense high pressure form of Sb_2O_3 (valentinite). A similar polytypic relationship probably exists for the two polymorphs of Sb_2O_3.

Some samples of Sb_2O_4 will be sent out of house for electron diffraction studies in an attempt to establish the polytypic relationship of α-Sb_2O_4 and β-Sb_2O_4. Some additional experiments will be conducted to establish the high pressure boundary curve between α and β-Sb_2O_4.

[3/] Most of the polymorphism study of Sb_2O_4 was conducted prior to the issuance of Interagency Agreement PR545160, and is included in this report for the sake of completeness.

2.4 The System Sb_2O_4-$KSbO_3$

This system has been examined between the compositional limits of $KSbO_3$ and Sb_2O_4. Sixteen compositions were studied by conventional quenching techniques and the materials were examined by powder and by single crystal x-ray diffraction techniques. Compositions which were initially calcined at 500 and 700°C for 60 hrs, were dried at 230°C for 1 hr, sealed in Pt tubes and reheated. The results of the experiments are given in the data presented in Table 5 from which the subsolidus relationships have been established as shown in Figure 4. The compound $KSbO_3$ with an ilmenite structure has been previously reported [9]. A body centered cubic solid solution phase originally reported as $KSbO_3$ [9] has been found to occur metastably at about 47.5% K_2O. The $3K_2O:5Sb_2O_5$ compound reported previously [10,11] was found in this work to melt congruently at about 1400°C. The $K_2O:2Sb_2O_5$ compound reported previously [11] was found in this work to have a phase transition at about 1000°C and to dissociate to pyrochlore plus $3K_2O:5Sb_2O_5$ at about 1150°C. The low temperature form of this compound labeled $P2_1/c$ represents a monoclinic phase with a=7.178A, b=13.378A, c=11.985A and β=124°10'. Single crystals of this phase were grown by flux evaporation from the composition $50K_2O:5Sb_2O_4:45MoO_3$. The unit cell and space group were determined from these crystals and confirmed by least square indexing of the powder diffraction pattern of the low temperature form of the compound $K_2O:2Sb_2O_5$. The pyrochlore solid solution exists at 1150°C from about 15 mole % K_2O:85 mole % Sb_2O_4 to greater than 30 mole % K_2O:70 mole % Sb_2O_4. The melting characteristics of these phases have been partially determined and are currently being reported.

2.4.1 Hyroxyl Ion Stabilization of Cubic Potassium Antimonate

The compound $KSbO_3$ was reported previously [12] as being cubic at ambient conditions when previously subjected to high temperatures and pressures. In this work two experiments were conducted, heating single

phase $KSbO_3$ ilmenite in sealed platinum tubes at about 750°C and 88,000 psi, utilizing argon as a pressure medium. The first of these, a two-hour run, showed only one small cubic line in the x-ray pattern but the specimen quickly reacted with atmospheric moisture. This experiment was then repeated for a longer time, 7 hours. In this time the material apparently reacted with the sealed Pt tube. The specimen was ground, mixed with petroleum jelly, and subjected to x-ray diffraction analysis before too much hydration could take place. The x-ray pattern showed lines of a material not seen by us previously. It may be concluded that this is a somewhat reducing environment and some of the material has transformed to K_2O and Sb_2O_3 which in turn melted and reacted with the Pt container.

The body centered cubic phase was not formed at the above stated conditions. However, occasionally small amounts of a cubic phase were seen in the x-ray powder diffraction pattern of $KSbO_3$ ilmenite heated at ambient pressure. For these reasons specimens of 1:1 and 3:5 mole ratios $K_2O:Sb_2O_4$ were equilibrated in air at 750°C for 60 hours and picked up oxygen to form the phases $KSbO_3$ and $K_3Sb_5O_{18}$ and then were reheated for one hour at 1200°C to drive off all excess moisture. X-ray diffraction patterns of these specimens showed single phase ilmenite and the $3K_2O:5Sb_2O_5$ compound. Portions of these 1200°C calcines were then weighed and mixed in acetone in the appropriate ratios to yield compositions of 46, 47, 47.5, 48 and 49 mole % K_2O. Each of these specimens was dried at 240°C for one hour and heated in open Pt tubes at 1200°C for one hour. Only the x-ray pattern of the 46% specimen showed a little $3K_2O:5Sb_2O_5$, the others contained only the cubic phase. A new specimen of 48 mole % K_2O was prepared in the same way except the Pt tube was sealed. After one hour at 1200°C, the x-ray pattern of the specimen showed only about 50% cubic. A new specimen of 48% was prepared by weighing the 1:1 and 3:5 phases immediately after removal from the

1200°C furnace and sealing the material in a flattened Pt tube within 1-2 minutes. This tube was then inflated at 1200° for a few minutes and the material mixed by shaking in a "wiggle-bug". The sealed specimen was then heated for 64 hours at 1200°C. The resultant specimen had exceedingly large grain growth indicating considerable solid state recrystallization but showed no cubic phase. The conclusion is inescapable that access to atmospheric moisture is probably necessary for the formation of the cubic phase at atmospheric pressure.

A paper entitled "Flux Synthesis of Cubic Antimonates" was published by the present authors during the course of this work [13]. In addition to the discovery that the F^- ion stabilized the formation of the body centered cubic phase of potassium antimonate it was disclosed that the cubic antimonate could also be obtained by reacting $KSbO_3$ with a small amount of other cations with small radii like B^{+3}, Si^{+4}, etc. It now appears obvious that in this reaction the boron or silicon (etc.) actually ties up some of the K^+ ion in a second phase and allows the K^+ deficient antimonate to react with atmospheric moisture to form the cubic antimonate previously thought to be "$KSbO_3$".

2.5 The System Sb_2O_4-$NaSbO_3$-NaF

2.5.1 The System $NaSbO_3$-NaF

To determine if NaF additions will stabilize the body-centered cubic phase similar to the $6KSbO_3$:KF-phase, NaF was added to $NaSbO_3$ in the ratio of $3NaSbO_3$:NaF, $4NaSbO_3$:NaF, $5NaSbO_3$:NaF, and $6NaSbO_3$:NaF. The x-ray diffraction patterns of these specimens contained varying amounts of body centered cubic phase, ilmenite, and NaF. After heating at 750°C and 1000°C in sealed Pt tubes, the x-ray patterns showed only ilmenite and NaF, however at ∿1150°C all the compositions contained some body centered cubic-type phase. The compositions $3NaSbO_3$:NaF and $4NaSbO_3$:NaF, when heated in sealed Pt tubes at ∿1250°C, did not contain ilmenite and

appeared to be the closest to single phase cubic. The small crystals of $4NaSbO_3$:NaF prepared by quenching in a small sealed tube appeared to be well formed truncated octahedrons. However, the room temperature x-ray diffraction pattern of the material had somewhat diffuse lines with the exception of the h00 lines which were reasonably sharp, suggesting rhombohedral symmetry. This material was placed on a hot stage microscope slide and analyzed by x-ray diffraction from room temperature up to 220°C. At 190°C the material appeared to start to go cubic and by 220°C a good quality cubic x-ray diffraction pattern was obtained (a=9.353A). When the material was cooled to room temperature the symmetry was again non-cubic. As the h00 lines deteriorate somewhat on cooling, the true symmetry of the room temperature form is probably no higher than monoclinic or triclinic rather than rhombohedral. It was therefore not unreasonable to expect that a body centered cubic phase could be obtained by direct synthesis with NaF without the necessity for Na^+ ion exchange.

2.5.2 The Ternary System

X-ray diffraction patterns (single crystal and powder) of selected NaF-flux synthesized (see Section 2.8.2.4) washed crystals show only a truly cubic bodyccentered phase (a=9.334A). It must be postulated that the composition formed by this technique is slightly different from that made essentially single phase at $4NaSbO_3$:NaF in a sealed tube. In an attempt to obtain a fluorine-substituted body centered cubic phase which exists at room temperature the compositions shown in Table 6 were prepared and show the reported phases when quenched from 1250°C. Equilibrium was not obtained in overnight heat treatments at 1200°C. At 1350°C the body centered cubic phase started to decompose. The composition $68NaSbO_3$:$4Sb_2O_4$: 28NaF (mole percent) was chosen as the best composition for further studies on ceramic procedures (Section 2.7).

The phases found in the specimens heated at ~1250°C are summarized in "equilibrium" diagrams for the quaternary system $NaSbO_3$-Sb_2O_3-Sb_2O_5-NaF (Figure 5) and the ternary plane of this system $NaSbO_3$-Sb_2O_4-NaF (Figure 6).

2.6 Other Systems

During the course of this study other alkali-oxide systems were surveyed, to decide whether interesting phases existed in these systems. Among those investigated were sodium and potassium bismuthates and sodium and potassium with several rare earth oxides, Nd_2O_3, Sm_2O_3, and Gd_2O_3 as well as with Y_2O_3.

2.6.1 Alkali Bismuthates

Samples of sodium bismuthates and potassium bismuthates were prepared from the respective alkali carbonates and Bi_2O_3 and heated in open Pt tubes at 500°C for various periods of time (Table 7). X-ray diffraction patterns showed essentially single phase Bi_2O_3 with several small unidentified peaks in the Na_2O-Bi_2O_3 samples. These peaks did not correspond with those of commercial $NaBiO_3$ (apparently prepared according to Scholder and Stobbe [14]), which decomposes to Bi_2O_3.

2.6.2 Alkali-Rare Earth Systems

Alkali carbonates were dry mixed with the respective rare earth oxides and heated as shown in Table 8. X-ray diffraction patterns were recorded with Ni filtered Cu radiation. A "?" indicates an unknown phase which is present as one or two small peaks in the pattern.

The only significant result of these studies appears to be the presence of the cubic rare earth structure in Gd_2O_3 well above its equilibrium transition. Apparently the alkali ion enters the rare earth oxide lattice to some extent, altering the polymorphic conditions.

2.6.3 Further Studies in the System Nb_2O_5:$KNbO_3$

During the interim between this contract and the previous one, it became apparent that the compound $2K_2O:3Nb_2O_5$ might have interesting ionic conductivity. However, as the exact ratio $40K_2O:60Nb_2O_5$ did not yield a single phase, new compositions were prepared (Table 9) and the composition $41K_2O:59Nb_2O_5$ was further studied. The conclusion that this is probably a non-stoichiometric phase led to a revision of the Nb_2O_5-$KNbO_3$ phase diagram (Figure 7).

2.7 Pellet Fabrication

2.7.1 $41K_2O:59Nb_2O_5$ ("2:3", $K_4Nb_6O_{17}$)

Evaluation by LeRC of the never-hydrated single crystal of $K_4Nb_6O_{17}$ supplied by NBS resulted in a request for single phase, polycrystalline, never-hydrated pellets of this same composition.

The starting material was prepared by dry mixing $KNbO_3$ and Nb_2O_5 in appropriate amounts, followed by calcining at 800°C for 10 hours and 1000°C for 30 hours with intermediate grinding. Pellets were pressed without binder at 10,000 psi in a 5/8 inch diameter steel die. Sintering was done in air at 1125°C for 18 hours. The pellets were removed from the sintering furnace at temperature, immediately placed in a silica glass tube, evacuated to $p \approx 2 \times 10^{-5}$ torr and sealed for transmittal.

The composition $2K_2O:3Nb_2O_5$ ($K_4Nb_6O_{17}$) was observed to contain a small amount of the tetragonal tungsten bronze (TTB) second phase. This second phase was completely eliminated by using a starting composition of $41K_2O:59Nb_2O_5$. A large batch of this 41:59 K/Nb composition was prepared and successfully exchanged as shown in Table 10. A pellet of the unexchanged 41:59 composition was prepared and sintered at 1100°C for 1 hour and subsequently exchanged. However, the problem of hydration with the 41:59 composition is much more severe than with the 2:3. It was necessary to maintain the sample at temperatures $\approx$ 100° - 150°C to obtain a powder diffraction

pattern and to our dismay, the exchanged pellet hydrated and decrepitated while being x-rayed in laboratory air. More elaborate precautions were necessary to successfully characterize pellets of this composition. It is not known if the lack of the TTB second phase increased the susceptibility to hydration or if this is due to a slightly higher than stoichiometric amount of K^+ (Na^+ in the exchanged material) in the lattice.

A series of heating experiments was performed to determine the optimum sintering conditions for pellets of nominal composition $41K_2O:59Nb_2O_5$. At a temperature of 1100°C overfiring of the pellet was pronounced, as evidenced by the presence of a small amount of a liquid phase and marked reduction of niobium. Attempts to reoxidize the sample by annealing at lower temperatures were not completely successful. Temperatures of 1000° and 1040°C (the melting point of $KNbO_3$) did not result in sintering sufficient to develop any mechanical strength. A temperature of 1050° and 2 hours time was found to result in sound pellets. X-ray characterization of the material after this heat treatment showed only single phase "2:3".

As stated above, the problem of hydration in this composition is severe at all stages of the fabrication and exchange. The following schedule was adopted in order to minimize the exposure to laboratory air, with each subsequent fabrication step performed with a minimum of delay.

Single phase $41K_2O:59Nb_2O_5$ powder → prepress 700 psi → isostatically press 20,000 psi → dry at 220°C 0.5 hr →

sinter at 1050°C 2 hrs → place in fused quartz tube, evacuate to $p \leq 10^{-5}$ torr and seal off

A similar procedure was used for the pellets to be exchanged, except that at the completion of sintering, the pellets were placed individually in

$NaNO_3$ and exchanged at 450°C for 64-68 hours. At the completion of the exchange period, the excess $NaNO_3$ was removed by leaching in methyl alcohol, the pellets were dried at 200°C for 0.5 hours and then placed in a fused quartz tube, evacuated and sealed.

During the exchange period, the pellets appeared to suffer no physical degradation and x-ray powder diffraction of a sample obtained from the center of a test pellet showed that complete exchange to the Na^+ phase had occurred.

Six pellets of the "2:3" K^+ phase and three pellets of the exchanged "2:3" Na^+ phase have been submitted for evaluation.

2.7.2 $4Rb_2O:11Nb_2O_5$ (11-layer phase)

Pellets of the 4:11 composition were prepared by using 1 weight percent stearic acid as a binder, pressed in steel dies at 10,000 psi and sintered at 1200°C in air for 56 hours. The pellets were sound and showed little tendency to spall or disintegrate during exchange in molten KNO_3 (see Table 10).

2.7.3 Large Pellets for Ionic Conductivity Measurements

As mentioned several times, the problems of hydration and compositional changes resulting from volatility or change in oxygen content in the alkali niobates, tantalates and antimonates necessitate the use of rather extreme measures to produce sound pellets. The complete encapsulation of the starting composition at the earliest stage possible in the fabrication process appears to be successful in some cases. In such cases, the specimen remains encapsulated until ready for evaluation.

Two compositions were prepared for large dense specimens to be sent to LeRC, $41K_2O:59Nb_2O_5$ and $NaSbO_{3-x}F_x$. The $NaSbO_{3-x}F_x$ was prepared by holding $7Sb_2O_4$:93KF at ∿1000°C for less than 10 minutes and then

separating the fines from the coarser grains by washing, settling, and centrifuging the insoluble product. The fines were then ion exchanged two times with $NaNO_3$ at 450°C - 2 hrs. The exchanged phase ($NaSbO_{3-x}F_x$) gave an x-ray pattern which was single phase cubic. The powders were pressed into 3/4" diameter pellets which were repressed isostatically at 20,000 psi. These pellets were placed in platinum envelopes, sealed on three sides and were again isostatically pressed to remove most of the air from the container. The envelopes were sealed and sent to a commercial company for isostatic hot pressing at ∿1100°C and 5,000 psi. The $41K_2O:59Nb_2O_5$ specimen was submitted to LeRC, unopened, in the platinum envelope. Duplicate specimens were used to determine physical integrity and phase composition of the pellets. The $NaSbO_{3-x}F_x$ specimen was not single phase after hot pressing, apparently as a result of decomposition under pressure. Three phases were evident: a cubic phase, the pyrochlore solid solution and NaF. It was felt that the exchanged product had a composition too close to a phase boundary with resultant instability under pressure. For this reason, it was decided to directly react the constituents to form the desired sodium containing phase directly and then hot press the product. A composition of $68NaSbO_3:4Sb_2O_4:28NaF$ was chosen.

Attempts to fabricate a large, dense specimen of the composition $68NaSbO_3:4Sb_2O_4:28NaF$ were largely unsuccessful. Direct reaction of the components at 750°C for 60 hours and 1000°C for 1 hour in open containers, with periodic grindings, resulted in a product containing $NaSbO_3$ (ilmenite) and a trace of NaF. Calcining temperatures as high as 1265°C were required to form a single phase material of the desired cubic structure. A trace of NaF was always present as a second phase. The use of such high calcining temperatures results in a coarse-grained product which could not easily be ground fine enough to produce a sinterable powder. Attempts to hot press the specimens in platinum envelopes,

using the same technique described above for the 41:59 and $KSbO_{3-x}F_x$ specimens, at a temperature of 1250°C for 10 minutes were unsuccessful. It is recommended that if these experiments are repeated, only the lower temperature calcines (at 750° and 1000°C) should be used, and the final desired phase in the pellet be produced by appropriate choice of time and temperature of hot pressing.

2.8 Crystal Growth and Synthesis

Many of the phases discovered during the phase equilibria studies of the alkali tantalate, niobate and antimonate systems have not been previously reported in the literature. One of the objectives of the crystal growth portion of the study has been to synthesize and grow small single crystals for x-ray diffraction studies to provide structural information on these materials and assist in the interpretation of x-ray diffraction powder patterns. The second, and equally important objective, has been to grow single crystals of the potentially useful K^+ and Rb^+ phases for use in studies of ion exchange behavior for the purpose of obtaining Na^+ phases. These studies are described in Section 2.9 of this report.

In general the choice of technique was dictated by the characteristics of the desired phase, i.e. congruent or incongruent melting, volatility of one or more components of the phase, range of coexistence with liquid, and desired final size of crystal. Both fluxed melt and Czochralski techniques were utilized, and in some cases, the flux evaporation technique was used for the preparation of small crystals.

2.8.1 Crystal Growth by Pulling from the Melt

2.8.1.1 Hexagonal Tungsten Bronze in the K_2O-Ta_2O_5-WO_3 System

Selective phase equilibria experiments with mixtures of $KTaO_3$ (KT) and WO_3 in the neighborhood of KT:$2WO_3$ (K_2O:Ta_2O_5:$4WO_3$) during the previous contract confirmed the existence of a hexagonal tungsten bronze (HTB)

structure. Single phase compositions were easily prepared between the pyrochlore composition, $K_2O:Ta_2O_5:WO_3$, and a composition $KTaO_3:3WO_3$ where a second, unidentified phase appeared. At the same time, exploratory crystal growth runs at lower Ta_2O_5 contents were encouraging and gave some promise of adaptation to the accelerated crucible rotation technique (ACRT) for single crystal growth of this bronze structure. However, considerably more work is required to determine the liquidus surface and primary field extent before such experiments would be definitive.

A 50 gram batch of $26.6K_2O:3.3Ta_2O_5:70.1WO_3$, prepared from KT, K_2WO_4 and WO_3 was premelted by induction heating in a platinum crucible. The crucible was then covered and transferred to a growth furnace. Following a 10 hour soak at 1200°C, the temperature was lowered at 2.5°C hr^{-1} to 500°C and the crucible removed from the furnace. Results were essentially the same as obtained in previously reported work with a cooling rate of approximately 30° hr^{-1}. Crystals were in general small, the largest ranging from about 6x6x0.2 mm to 3x3x0.1 mm. The yield, based on visual estimate, was small.

Because of the small total yield and extensive nucleation and growth of small platelets, an attempt was made to pull crystals of the HTB from the fluxed melt. A 250 gram charge of composition $27K_2O:5Ta_2O_5:68WO_3$ was placed in a platinum crucible in a growth furnace which was baffled to provide an essentially isothermal chamber except directly above the center of the melt where the platinum pull rod was inserted. The charge was held at 1225° for three hours prior to attempting growth. Although no evidence of solid was present on the surface of the melt, extensive freezing of polycrystalline material occurred when the pull rod was inserted. The temperature was raised in increments and the polycrystalline mass redissolved. All attempts to achieve growth were unsuccessful at temperatures up to 1250°.

In the final attempt, at 1265°C, crystallization on the pull rod was slow enough to allow a 16 hour pull. X-ray diffraction examination of the results indicated that the crystals obtained were the desired phase. However, physically, the crystals were in the form of small plates, bound together by the frozen melt. It appears that a considerable effort would be required to establish suitable conditions for the growth of larger single crystals of this HTB. This would probably require a minimum of 1-2 man years.

2.8.1.2 The System $KNbO_3$-Nb_2O_5

Single crystals of $K_4Nb_6O_{17}$ have rather easily been grown both at other laboratories [15] and at NBS. However, the material hydrates readily in laboratory air with subsequent degradation of the crystalline perfection, which is not regained by drying. In order to provide LeRC with a large single crystal which had never been hydrated, a crystal was grown from a melt of the same composition, removed from the puller while still at a temperature of 300-400°C and immediately placed in a fused silica ampoule, evacuated to $p \leq 2 \times 10^{-5}$ [4/] torr and sealed for transmittal. Later conversations with LeRC indicated that the behavior of this crystal was indeed different, and as described in the section on pellet preparation, never hydrated pellets were also supplied for evaluation.

2.8.1.3 The System Rb_2O-Nb_2O_5

A 100 gram batch of $29Rb_2O:71Nb_2O_5$ was calcined at 400° for 60 hours and used for crystal pulling experiments. Five single and/or polycrystalline boules of the 4:11 (Rb:Nb) (11-layer) hexagonal phase were pulled from the melt by the top seeded solution method. The crystals were obtained using both seeded and unseeded pull rods. These crystals were used as "purified" material for the growth of single crystal 11L for use as a stable end member of the system and for chemical analysis.

[4/] The use of torr follows the current common practice of workers in the field. Note that 1 torr = 1.32×10^{-3} atm = 1.34×10^2 N/m^2.

The crystals appear to be susceptible to thermal shock and therefore must be cooled relatively slowly. Self-seeded crystals show a marked preference for growth perpendicular to the c-axis. At least one excellent cleavage (basal-plane) is evident.

Crystals of the hexagonal tungsten bronze (HTB) phase in this system ($21.75Rb_2O:78.25Nb_2O_5$) were grown by pulling from a melt of the same composition (experiments performed by C. Jones while on an American University Research Participation Program). Large, clear water-white crystals were easily obtained but all fractured into rather large blocks upon cooling. All attempts to prevent cracking were unsuccessful and the cause remains unknown, but may be related to a symmetry change to orthorhombic on cooling.

Crystals of the Gatehouse tungsten bronze (GTB) ($11.5Rb_2O:88.5Nb_2O_5$) phase were grown from a melt of composition $16Rb_2O:84Nb_2O_5$ (experiments performed at NBS by D. Klein while on an American University Research Participation Program). Small single crystal boules were successfully grown, but again fractures developed as soon as the boules were removed from the melt at the completion of the run in spite of all attempts at slow cooling of the boule.

2.8.2 Flux Growth

2.8.2.1 The System Rb_2O-Nb_2O_5-MoO_3

Nine different compositions in this system were prepared (2 gm batches) and heated by induction to temperatures in the 900°-1100°C range in small platinum crucibles. Recrystallization and/or volatility of the MoO_3 resulted in the formation of small crystals. Crystals (2mm+) of the 11 layer hexagonal (4:11) phase were obtained from compositions of $30Rb_2O:5Nb_2O_5:65MoO_3$ and $30Rb_2O:10Nb_2O_5:60MoO_3$. A $27.5Rb_2O:10Nb_2O_5:62.5MoO_3$ composition yielded small crystals of the GTB

phase (~11.5 mole % Rb_2O) and H-Nb_2O_5 and $28Rb_2O:5Nb_2O_5:67MoO_3$ yielded small single crystals of the HTB (~21.75 mole % Rb_2O). No crystals of the unidentified phase occurring at about 15 mole % Rb_2O in the binary system were obtained with any MoO_3 flux composition. This is further reason to believe this phase may not be an equilibrium compound in the binary system.

2.8.2.2 The System Rb_2O-Ta_2O_5-MoO_3

Six different compositions were prepared in the ternary system for flux evaporation crystal growth. Single crystals of the 9 layer phase (1:3) were grown using compositions of $30Rb_2O:10Ta_2O_5:60MoO_3$ and $35Rb_2O:5Ta_2O_5:60MoO_3$. Crystals of the other phases in the binary system Rb_2O-Ta_2O_5 could not be obtained using this method, probably because their primary fields do not extend to such high MoO_3 contents, or to the relatively low temperatures involved.

2.8.2.3 The System Rb_2O-Ta_2O_5-RbF

In view of the success obtained by the flux synthesis route in the $KSbO_3$-KF system [13] similar attempts were made using RbF and Ta_2O_5. A $95RbF:5Ta_2O_5$ composition was completely liquid at about 925°C and on cooling yielded acicular crystals of an unknown phase. A $75RbF:25Ta_2O_5$ composition was heated to about 1150°C for 30 seconds and quickly cooled. After leaching with water, a sizeable yield of clear, well-formed, octahedral crystals of the $RbTa_2O_5F$ pyrochlore phase was obtained.

2.8.2.4 The Systems $ASbO_3$-Sb_2O_4-AF (A = Na,K,Rb)

The techniques for synthesis and growth of small crystals of $KSbO_{3-x}F_x$ by reaction between KF and Sb_2O_5 at temperatures in the 1000°C range, developed during this contract, have been described [13].

Attempts were made to melt the flux-synthesized $KSbO_{3-x}F_x$ in air with the thought it might be possible to pull crystals directly from

a melt of that particular composition. The material decomposed as the melting point was reached, indicating that pulling in air would not be feasible. A large batch of ∿50 grams was prepared with a composition of $70KF:30Sb_2O_4$ and heated in an effort to obtain a melt (single phase liquid) suitable for crystal pulling. At all temperatures below which there was excessive volatilization a solid phase remained. It seems obvious now that we have to go much higher in KF concentration to obtain a composition which may be suitable for crystal growth.

Quenching experiments indicated that mostly ilmenite was formed at temperatures up to ∿1200°C in the system $NaF-NaSbO_3$. We decided to attempt a direct synthesis of the sodium cubic phase in the same manner as for the $KSbO_{3-x}F_x$ but at a higher temperature. A 3 gram batch of $NaF-Sb_2O_4$ (molar ratio 93:7) was heated in a platinum crucible to 1250°C and the NaF allowed to evaporate for 35 minutes. After leaching the residue in water we obtained essentially single phase $NaSbO_{3-x}F_x$.

The largest crystals were of the order of 1 mm. Some flat hexagonal plates of ilmenite are formed at the lip of the crucible, probably during volatilization of the sodium antimony fluor-oxide, however these can easily be separated mechanically from the cubic phase.

X-ray diffraction patterns (single crystal and powder) of selected washed crystals show only a truly cubic body centered phase (a=9.334A). It must be postulated that the composition formed by this techique is slightly different from that made essentially single phase at $4NaSbO_3:NaF$ in a sealed tube.

Exploratory flux evaporation heatings were made in the $KSbO_3-Sb_2O_4-KF$ and $RbSbO_3-Sb_2O_4-RbF$ systems as a preliminary step in the determination of suitable starting compositions for flux crystal growth of the desired $ASbO_{3-x}F_x$ phases. The results are summarized

in Table 11. None of the reported compositions would appear to be suitable for top-seeded solution growth both from the standpoint of the excessive volatility of the alkali fluoride at the temperatures involved and the presence of a solid phase. The presence of a solid phase at such high concentrations of flux (alkali fluoride) indicates that either a gradient transfer technique in sealed crucibles must be adopted or the suitability of other flux systems investigated.

An attempt was made to synthesize "$RbSbO_3$" in the cubic polymorph by direct flux synthesis from the composition $95RbF:5Sb_2O_4$ heated for one hour at about 900-1000°C in an open Pt crucible. Well developed psuedo-octahedral crystals were formed and easily isolated although their exact composition is unknown. However single crystal x-ray diffraction patterns indicated that these crystals were probably triclinic, although the observed unit cell was C-centered.

2.9 Ion Exchange

One of the the best screening tests for ionic conductivity of a solid phase is to determine whether or not the alkali ion in the structure can be exchanged with an alkali ion of a different species. This may be tested by heating in a large excess of a molten salt (or solution) containing the second ion. A large number of experiments of this type were performed on many different compounds found in this and the previous year's [1] study. The results of these tests are found in Table 10(a).

Most of the exchange experiments have been performed on powdered materials. In those cases where single crystals could be grown either by flux techniques or melt techniques (see Section 2.8), attempts were also made to ion exchange the single crystals.

In general, the results of ion exchange experiments on single crystals were disappointing in that either disruption of the single crystal

occurred or exchange proceeded at extremely low rates. Thus it appears that a study of technique development for ion exchange of single crystals would be appropriate if these are to be useful in device applications. Consideration should be given to the use of an electric field or other technique in order to obtain a greater driving force for exchange.

Ion exchange experiments were conducted in the Rb_2O-Nb_2O_5 system with particular emphasis on the 11-layer compound occurring at or about $4Rb_2O$:$11Nb_2O_5$ (26.67 mole % Rb_2O). Ion exchange experiments were conducted on both single crystal fragments obtained from crystals grown from the melt and low temperature calcines of 4:11 powders. The single crystals underwent K^+ exchange in molten KNO_3 but disintegrated during Na^+ exchange in $NaNO_3$ during various temperature and time combinations. Pellets of the 11-L phase were pressed both uniaxially and isostatically with and without polyvinyl alcohol binder. Pellets were fired and x-ray patterns made before any attempt was made to induce ion exchange. Generally the K^+ exchange occurred without too much degradation of the specimen but the pellets disintegrated to a fine powder during Na^+ exchange. Results of these exchange experiments are also presented in Table 10.(b). The unit cell dimensions for complete ion exchange were developed from ion exchange in molten salts from very small single crystal fragments.

3.0 RELATION OF STRUCTURAL MECHANISMS OF NON-STOICHIOMETRY TO IONIC CONDUCTIVITY

It is probably generally accepted that a phase which exhibits unusual ionic conductivity must necessarily be structurally non-stoichiometric. Unfortunately the opposite is not necessarily true. Nevertheless a crystallographic understanding of non-stoichiometric phases is an obvious necessity to the tailoring of new fast-ion conductors. For this reason it is worthwhile to discuss the nature of the non-stoichiometry which has been observed in this study for those phases which seem to be of interest.

3.1 Hexagonal Tungsten Bronze-type Phases (HTB)

It has already been mentioned in the previous summary report [1] that the hexagonal tungsten bronze-type phase (HTB) found in binary alkali niobate and tantalate systems has alkali ions in non-stoichiometric positions and excess Nb^{+5} or Ta^{+5} ions. These excess pentavalent ions may well block the alkali ion conductivity as these hexagonal bronzes cannot be ion exchanged. There are two mechanisms that have proved effective in altering the ion exchange characteristics of the hexagonal tungsten bronze-type structures. One is to change the total alkali:other cation valence ratio by substituting W^{+6} for Ta^{+5}, for instance in the system $KTaO_3$-WO_3. In this case the HTB phase occurs at about the 1:2 ratio and the K^+ ion can be replaced with Na^+ by heating in a large excess of $NaNO_3$. Unfortunately the Na-tantalum-tungstate is not stable above about 450°C and therefore cannot be formed into low porosity ceramics by conventional techniques. The single crystals of HTB grown with the potassium tungstate flux (Section 2.8.2.1) need some greater driving force then temperature (<450°) to obtain complete exchange with Na^+ ions. The alternate to replacing Ta^{+5} ions with W^{+6} ions is to change the structure enough to allow ion exchange (See Section 3.3).

3.2 Pyrochlore Phases

In the $KTaO_3$-WO_3 system a pyrochlore phase also occurs at about the 1:1 ratio or $K_{1.0}[TaW]O_6$. Unfortunately the pyrochlore in this system transforms to a tetragonal tungsten bronze (TTB) at high temperatures. Although it can be ion exchanged with Na^+, this pyrochlore phase also is not stable above about 450°C. The only stable Na^+ containing pyrochlore is the one in the Sb_2O_4-$NaSbO_4$ system and apparently this one is not a good ionic conductor.

The distribution of Na^{+}, Sb^{+3}, Sb^{+5} and O^{-2} ions in a pyrochlore single crystal is currently under evaluation by the Crystallography Section at NBS. However, certain assumptions can be made which may enable us to postulate the approximate distribution. The formula for the compositions observed to result in a pyrochlore structure might be postulated to be $[NaSb^{+3}]Sb_2O_7$ for the Na/Sb ratio of 1:3, $[Na_{1\ 1/3}Sb^{+3}_{2/3}]Sb_2O_{6.67}$ for 1:2, and $[Na_{1\ 1/2}Sb_{1/2}]Sb_2O_{6.5}$ for 3:5. However, these compositions do not illustrate the structural nature of pyrochlore nor account for the observation that the "lone pair" electrons associated with Sb^{+3} will not allow O^{-2} ions to completely coordinate the antimony and result in apparent vacancies.

The structural formula of pyrochlore should be written as $[A_2X]\ [B_2X_6]$ to emphasize the fact that the octahedral network of B_2X_6 is required to be complete if the structure is to be stable. The A_2X ions fill the intersecting channels in this B_2X_6 framework. In our material the B_2X_6 framework must be represented as $[Sb^{+5}_2O_6]^{-2}$ and must be stoichiometric. All remaining Na^{+} and O^{-2} ions, as well as Sb^{+3}, must be in the $[A_2X]^{+2}$ portion of the formula. All Sb^{+5} must be in B_2X_6 and only Sb^{+3} in A_2X. Furthermore the maximum number of the sum of Na^{+1}, Sb^{+3} excess O^{-2} (beyond O^{-2}_6) and "lone pair" electrons cannot exceed three. One can then write the general formula as $[A_2O]^{+2}[Sb_2O_6]^{-2}$ with $[A_2O]^{+2}$ equal to

$$Na^{+1}_{2/k} + Na^{+1}_{x} + Sb^{+3}_{kx} + O^{-2}_{y} + \boxed{L.P}_{kx} \leq 3$$

where k equals the ratio Sb/Na. Using the ionic valences and the sum of the ions equal to three, maximum densities can be calculated and compared with the observed to test the structural hypothesis. The maximum density for the Na/Sb ratio of 1:3 represented by the formula $[Na^{+1}_{0.917}Sb^{+3}_{0.75}O^{-2}_{0.583}\square_{0.75}]^{+2}\ [Sb^{+5}_2O_6]^{-2}$ is calculated to be 5.469 units.

For the Na/Sb ratio of 3:5 with the formula $[Na^{+1}_{1.5}Sb_{0.5}O^{-2}_{0.5}\square_{0.5}]^{+2}\ [Sb_2O_6]^{-2}$ the density is calculated as 5.406. For the intermediate composition with the Na/Sb ratio of 1:2 and a formula of $[Na^{+1}_{1.294}Sb^{+3}_{0.588}O^{-2}_{0.529}\square_{0.588}]^{+2}\ [Sb_2O_6]^{-2}$ the maximum density is found to be 5.481. The density found for our isostatically hot pressed specimens is 96.0% of the maximum theoretical density. It should be remembered however that the true theoretical density of any given Sb/Na ratio will decrease with decrease in temperature. Thus the densities obtained on our hot pressed specimens are, in all probability, greater than 96% of theoretical in view of the expected increased oxidation of the Sb at the relatively low temperatures involved.

As stated above, the pyrochlore structural formula should be written as $[A_2X]\ [B_2X_6]$. The $RbTa_2O_5$ is apparently equivalent to the formula

$$[\square_2Rb]^{+1}\ [Ta_2O_5F]^{-1}$$

as shown by Hong's structural study [16] of single crystals prepared by the flux synthesis method described by NBS [17]. The Rb^+ ion is apparently too large for the A sites and it is this preference for the larger anion site that makes this compound stable. During ion exchange in KNO_3 the K^+ ion apparently enters the A site and, upon exposure to atmospheric moisture, an H_2O molecule occupies the site formerly containing Rb^+. The formula is then

$$[\square_K\ H_2O]^{+1}\ [Ta_2O_5F]^{-1}$$

During sodium exchange it is apparently possible to obtain a non-stoichiometric amount of Na in this lattice. The formula for this phase can probably be written as

$$[Na_{1+x}OH_x]^{+1}\ [Ta_2O_5F]^{-1}.$$

The product obtained by acid leaching of this pyrochlore is apparently

$$[\square_2 H_3 O]^{+1} [Ta_2 O_5 F]^{-1}.$$

Although infra-red analysis of the Na^+ exchange product does not indicate $(OH)^-$ [18] it would probably be worthwhile to examine this product with NMR for hydrogen resonance, a much more sensitive method than infra-red adsorption.

3.3 Hexagonal Tungsten Bronze - Pyrochlore Series

The $[B_2X_6]$ framework of the pyrochlore structure can be described as being made up of alternating layers of the hexagonal tungsten bronze structure separated by layers of isolated octahedra sharing only two corners with the adjacent HTB layers. If this structure is modified by increasing the sequence number of either of these types of layers from ABAB to AABAAB or AAABAAAB etc., a sequence of hexagonal phases would be formed having the same a axis as the HTB structure and with varying but integral multiplicities of the c axis dimension. Such phases are actually encountered in the K_2O-Ta_2O_5 [1,2] Rb_2O-Nb_2O_5 and Rb_2O-Ta_2O_5 systems and have been estimated by us to represent 9-layer, 16-layer and 11-layer sequences. All of the phases can be ion exchanged for Na^+ unlike the HTB in the same systems. The reason for this appears to be that a rotation or translation of a portion of the layer sequence allows the isolated vertical channels found in the HTB structure to be changed to intersecting channels as in the cubic pyrochlore structure. The exact crystallographic nature of these compounds is currently under investigation by Dr. B. T. Gatehouse at Monash University, Melbourne, Australia. Unfortunately, however, the Na^+ ion exchanged products are again not stable above about 450°C.

As is the case with the pyrochlore compounds the K_2O containing phases have unit cell dimensions very similar to or even larger than the corresponding Rb_2O containing phases. For instance the c-axis for

the 11-layer phase in the K_2O-Ta_2O_5 system is 43.512A while that in the Rb_2O-Nb_2O_5 system is 43.18A and in the Rb_2O-Ta_2O_5 43.19A. This may be due to a real difference in total alkali content. It may also be due to hydration of the K_2O phases. No high temperature x-ray data is available to check this hypothesis but small single crystals of the 2:5 K_2O:Ta_2O_5 phase have been noted to crack, spall and jump on exposure to air.

3.4 Body Centered Cubic Antimonates

A successful method of synthesizing cubic potassium antimonate by heating in molten KF was published by the present authors during this contractural period [13]. The major reason for the success in obtaining completely single phase fluorine stabilized cubic potassium antimonate is that the potassium ilmenite is H_2O soluble and may be easily separated from the cubic material.

An examination of the structural model of the octahedral framework of the body centered cubic antimonate phase suggests that this structure must always have some anion (X) occupancy in the 000, 1/2 1/2 1/2 position. The structural formula thus appears to be $[A_{16}X_2]^{+12}[Sb_{12}O_{36}]^{-12}$ with the alkali ion in position (A) located at (or just off) the juncture of the open cages. However, it seems very likely from both structural reasons (bond lengths, etc.) and valency considerations that either or both of the non-framework positions will be nonstoichiometric. Valency considerations require that at least two out of 16 alkali ions must be missing and the structural formula then be $[\square_2A_{14}X_2]^{+12}[Sb_{12}O_{36}]^{-12}$. This formula corresponds to the composition reported by the Lincoln Laboratory report [19] for the single crystal x-ray diffraction analyses of the phase synthesized with KF according to the NBS method [13]:

$$K_{12}Sb_{12}O_{36}.2KF \text{ or } [\square_2K_{14}F_2]^{+12}[Sb_{12}O_{36}]^{-12}.$$

It seems quite likely, however, that this general formula does not completely account for all of the preparations which have been observed to form this structure, whether body centered or primitive. The observation that a primitive phase can be formed, in air, by reaction with atmospheric moisture at a 48:52 ratio suggests that this phase may well have considerably less than 14 alkali ions per unit cell. The formula must be compensated, in this case, by a substitution of a monovalent anion (OH, F) in the octahedral framework. The general formula then becomes $[\square_{2+x}A_{14-x}X_2]^{+(12-x)}[Sb_{12}O_{36-x}X_x]^{-(12-x)}$.

The composition found at ∿48:52 in the potassium antimonate system can be written (assuming a ratio of 11:12 K/Sb or 47.826% K_2O):

$$K_{22}Sb_{24}O_{71}+5H_2O \rightarrow K_{22}Sb_{24}O_{66}(OH)_{10} \text{ or } [\square_5K_{11}(OH)_2]^{+9}[Sb_{12}O_{33}(OH)_3]^{-9}$$

which also can be described as $6KSbO_3:3Sb_2O_5:5KOH$ (see Figure 8). The general formula describing the K^+ containing compositions is then

$$[\square_{2+x}K_{14-x}X'_2]^{+(12-x)}[Sb^{+5}_{12}O_{36-x}X'_x].$$

The above formula contains only pentavalent antimony and apparently does not completely explain the compositions which form a 'stable' body centered cubic phase in the system $NaSbO_3:Sb_2O_{4+x}:NaF$. The only formula which does not involve the loss or gain of O^{-2} (or F^-) when the Sb_2O_4 is added in a sealed tube corresponds to:

$$[\square_2Na_{14}F_2][Sb^{+3}_ySb^{+5}_{12-y}O_{36-2y}F_{2y}]$$

which is represented by the join 6:1 -- 3:7 on Figures 5 and 6. There is really no place in the framework structure for Sb^{+3} and it is difficult to believe that octahedrally coordinated antimony can be Sb^{+3}. The lone pair electrons can be attached to the sodium ions instead of the antimony or just in the vacancies. However, for convenience, the

formulas can be written involving Sb^{+3}. The new formula would then have two variables:

$$[\square_{2+x}A_{14-x}X'_2] \quad [Sb^{+3}_{y}Sb^{+5}_{12-y}O_{36-(x+2y)}\ X'_{(x+2y)}]$$

represented by the plane in the quaternary system $NaSbO_3$:Sb_2O_3:NaF bounded by the 6:1 -- 3:4 and 6:1 -- 3:7 joins of Figures 5 and 6. However the single phase region in this system actually appears to contain more NaF than described by this general formula. Apparently some O^{-2} is evolved in the sealed Pt tubes, the amount depending on uncontrolled variables such as the amount of free volume in the tube and on changes from the original composition during treatment. The absolute maximum amount of NaF which can be accommodated structurally by the body centered cubic phase can be described by the formula

$$[Na_{16}F_2]^{+14}[Sb^{+3}_{2-x}Sb_{10-x}O_{34-2x}F_{2+2x}]^{-14}$$

which represents a line in the system shown by the join 3:1 -- 3:8 in Figure 6 and involves the evolution of one molecule of gas (O_2) per formula unit. The results of our investigations so far suggest that the body centered phase approaches this formula as a limit. The composition of the cubic phase in equilibrium with excess Sb_2O_4 and molten NaF actually appears to touch this line at approximately $10NaSbO_3$:Sb_2O_4:6NaF or

$$[Na_{16}F_2] \quad [Sb^{+3}_{3}Sb^{+5}_{9}O_{32}F_4] + O_2.$$

The single phase distorted cubic material on the binary join $NaSbO_3$:NaF appears to have a composition between 6:1 and 5:1 or approximately $11NaSbO_3$:2NaF or

$$[Na_{14.18}F_2]\ [Sb_{12}O_{35.818}F_{0.1818}] + .0909\ O_2.$$

The compositions in the quaternary system thus probably lie on a join between these two end members.

A large number of experiments were performed in an attempt to synthesize ceramic products of single phase body centered cubic sodium antimonate "stabilized" with F^+. Although we have not yet succeeded in preparing such a ceramic all indications point to a short time heat treatment with specific specimen preparation techniques. These almost unique conditions indicate that the body centered cubic phase is not really stable under the conditions at which it is formed. Thus either its true stability field may lie at some higher or lower partial pressure of O_2 (or OH) or it may always be metastable under any conditions.

3.5 The Phase $2K_2O:3Nb_2O_5$

In the previous contract summary report [1] it was reported that the compound occurring at about $2K_2O:3Nb_2O_5$ had the unit cell dimensions a=7.822, b=33.019, c=6.481A when not hydrated. Only the b axis expanded upon exposure to moisture as previously mentioned by Nassau [15]. From these unit cell dimensions several postulations can be made. The a direction corresponds to 2x3.911 or two O-Nb-O distances and probably represents two Nb-octahedra sharing oxygen at their corners. The c direction corresponds to 2x3.2405 or two times the O-O distance corresponding to edge sharing of the Nb-octahedra. The b direction is $\sim$10 times the value for edge sharing. It may be assumed that the structure is made up of layers or slabs perpendicular to b, composed of octahedra edge-shared in the c direction and corner shared in the a direction. These slabs must be separated by layers of K^+ ions and the K^+ ions should then be rather mobile. That this is actually the case is demonstrated by our reported ion exchange with Na^+ where the b axis changes to 30.78A and the conductivity measurements made by LeRC [20]. The actual crystal structure of this phase is currently under investigation by Dr. N.C. Stephenson of the New South Wales Institute of Technology, Sydney, Australia.

Although no ionic-conductivity or even ion exchange studies have been performed on the compound $K_2O:3Nb_2O_5$ it is sufficiently similar to the 2:3 phase to warrant some additional study.

4.0 SUMMARY OF RESULTS

1. Single crystals of hexagonal tungsten bronze (HTB) were synthesized in the system $KTaO_3$-WO_3-K_2WO_4 by the flux technique. No crystals large enough to measure conductivity by the presently utilized techniques were successfully obtained.
2. The phase equilibria up to and including the liquidus of portions of the systems Rb_2O-Nb_2O_5 and Rb_2O-Ta_2O_5 have been studied and phase diagrams have been constructed most consistent with the experimental data. Single crystals were grown of most of the compounds in the niobate system and the phases were investigated for ion exchange properties. Single crystal and polycrystalline specimens were submitted to the sponsor for evaluation.
3. The phase equilibria up to and including the liquidus of the systems Sb_2O_4-$NaSbO_3$ and Sb_2O_4-$KSbO_3$ have been studied and a phase diagram has been constructed most consistent with the experimental data. Polycrystalline ceramic specimens of the pyrochlore phase were prepared and submitted to the sponsor for evaluation.
4. The stabilization of cubic antimonates by addition of F^+ was studied in an attempt to provide a low porosity Na^+ ion ceramic specimen for evaluation. Although small single crystals were easily synthesized by the alkali fluoride flux technique, no crystals larger than $\sim$1-2 mm were obtained.
5. Many other alkali-oxide rare earth oxide and Bi_2O_3 systems were examined but no new interesting phases identified.
6. The phase occurring at about $2K_2O:3Nb_2O_5$ was found to have interesting ion exchange and ionic conductivity properties.

5.0 FUTURE WORK

1. Develop techniques to grow large crystals from a flux. Such techniques have only been reported for a very few phases and generally involve an inordinate amount of man hours to produce results.
2. Develop techniques to ion exchange large crystals, perhaps by utilizing an electronic current with a hot alkali salt or solution.
3. Investigate and develop improved fabrication techniques to produce dense, sound pellets of the $68NaSbO_3:4Sb_2O_4:28NaF$ composition in a size suitable for definitive ionic conductivity measurements and examine the effect of varying composition on conductivity.
4. Obtain crystallographic structure analyses on $2K_2O:3Nb_2O_5$ and on $4Rb_2O:11Nb_2O_5$ (now being conducted by N.C. Stephenson and B. Gatehouse).

References

1. R.S. Roth, H.S. Parker, W.S. Brower and D. Minor, Alkali Oxide-Tantalum Oxide and Alkali Oxide-Niobium Oxide Ionic Conductors, NASA Report No. CR-134599, April 1974.

2. R.S. Roth, H.S. Parker, W.S. Brower and J.L. Waring, "Fast Ion Transport in Solids, Solid State Batteries and Devices", Ed. W. vanGool. Proceedings of the NATO sponsored Advanced Study Institute, Belgirate, Italy, Sept. 1972, North Holland Publishing Company, Amsterdam (1973) pp. 217-232.

3. B.M. Gatehouse, D.J. Lloyd and B.K. Mishkin, "Solid State Chemistry" Proceedings 5th Materials Research Symposium, NBS Special Publication 364 (1972) 15.

4. N. Schrewelius, Diss. Stockholm (1943) pp. 144.

5. D.J. Stewart and O. Knop, Canadian J. of Chemistry 48 (1970) 1323.

6. J. Singer, NASA Lewis Research Center, Cleveland, Ohio, (personal communication).

7. K. Dihlstrom, Z. Anorg. Allgem Chem. 239 (1938) 57.

8. D. Rogers and A.C. Skapski, Proc. Chem. Soc. (1964) 400.

9. P. Spiegelberg, Ark. f. Kemi Min. och Geol. 14 [5] (1940) 1.

10. B. Aurivillius, Ark. f. Kemi 25 (1964) 505.

11. H. Y-P. Hong, Preprint from Lincoln Lab., MIT, sponsored in part by NASA Contract C-43205-C (1974).

12. J.A. Kafalas, "Solid State Chemistry", Proceedings 5th Materials Research Symposium, NBS Special Publication 364 (1972) 287.

13. W.S. Brower, D.B. Minor, H.S. Parker, R.S. Roth and J.L. Waring, Matl. Res. Bull. 9 (1974) 1045.

14. R. Scholder and H. Stobbe, Zeit. f. an. u. all. Chemie 247 (1941) 392.

15. K. Nassau, J.W. Shiever and J.L. Bernstein, Jr. Electrochem. Soc. 116 (1969) 348.

16. J.B. Goodenough, H. Y-P. Hong and J.A. Kafalas, Twelfth Monthly Report - NASA Contract C-43205-C (Aug. 1974).

17. R.S. Roth, H.S. Parker, W.S. Brower, J.L. Waring and D.B. Minor, February and March Monthly Letter Progress Reports, NASA Interagency Order C-50821-C (1974).

18. J.B. Goodenough, K. Dwight, H. Y-P. Hong and J.A. Kafalas, Fifteenth Monthly Report - NASA Contract C-43205-C (Nov. 1974).

19. J.B. Goodenough, H. Y-P. Hong and J.A. Kafalas, Ninth Monthly Report - NASA Contract C-43205-C (May 1974).

20. J. Singer, W. L. Fielder, H.E. Kautz and J.S. Fordyce, Bull. Am. Ceram. Soc. 54 (1975) 454.

Figure Captions

Figure 1. Phase equilibrium diagram for the system Nb_2O_5-$4Rb_2O$:$11Nb_2O_5$.

- ● - liquidus values from reference [21]
- o - completely melted
- ⊖ - partially melted
- x - no melting

Figure 2. Phase equilibrium diagram for the system Ta_2O_5-$4Rg_2O$:$11Ta_2O_5$.

- ⊖ - partially melted
- ● - no melting

Figure 3. Phase equilibrium diagram for the system Sb_2O_4-$NaSbO_3$. Not necessarily a true binary system. (L = liquid, S = solid, V = vapor)

- ● - melting
- x - no melting

Figure 4. Phase equilibrium diagram for the system Sb_2O_4-$KSbO_4$. Not necessarily a true binary system.

- ● - melting
- x - no melting
- ss - solid solution
- 1:2 - K_2O:$2Sb_2O_5$
- 3:5 - $3K_2O$:$5Sb_2O_5$
- $P2_1/c$ - low temperature form of K_2O:$2Sb_2O_5$

Figure 5. Phase relations in the quaternary system $NaSbO_3$-Sb_2O_3-Sb_2O_5-NaF.

The join 6:1--3:4 represents the formula

$$[\square_{2+x}Na_{14-x}F_2]\ [Sb^{+5}_{12}O_{36-x}F_x]$$

The join 6:1--3:7 represents the formula

$$[\square_{2}Na_{14}F_2]\ [Sb^{+3}_{y}Sb^{+5}_{12-y}O_{36-(x+2y)}F_{(x+2y)}]$$

Figure 6. Phase relations in the ternary system $NaSbO_3$-Sb_2O_4-NaF

The join 6:1--3:4 represents the formula

$$[\square_{2+x}Na_{14-x}F_2]\ [Sb^{+5}_{12}O_{36-x}F_x]$$

The join 6:1--3:7 represents the formula

$$[\square_2 Na_{14} F_2]\ [Sb_y^{+3} Sb_{12}^{+5} O_{36-(x+2y)} F_{(x+2y)}]$$

The join 3:1 --3:8 represents the formula

$$[Na_{16} F_2]\ [Sb_{2+x}^{+3} Sb_{10-x}^{+5} O_{34-2x} F_{2+2x}] + O_2$$

Figure 7. Phase equilibrium diagram for the system Nb_2O_5-$KNbO_3$

x - liquidus values from reference [22]
o - completely melted
⊖ - partially melted
● - no melting

Figure 8. Representation of the ternary system $KSbO_3$-Sb_2O_5-KOH illustrating the hydration of the 11:12 mixture to form the single phase cubic compound when heated in air.

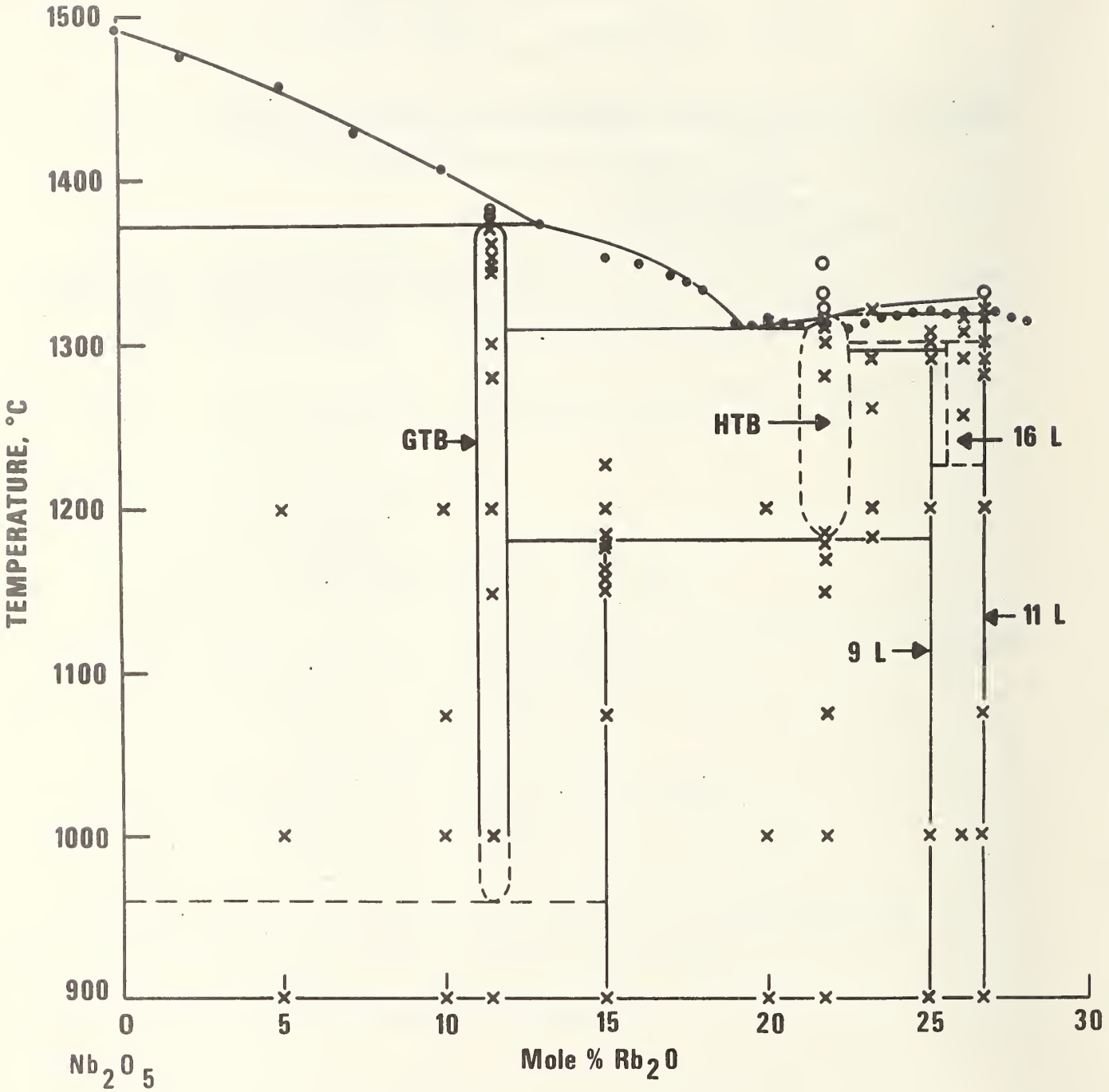
1500
1400
1300
1200
1100
1000
900
TEMPERATURE, °C
GTB
HTB
16 L
11 L
9 L
0
5
10
15
20
25
30
Nb_2O_5
Mole % Rb_2O

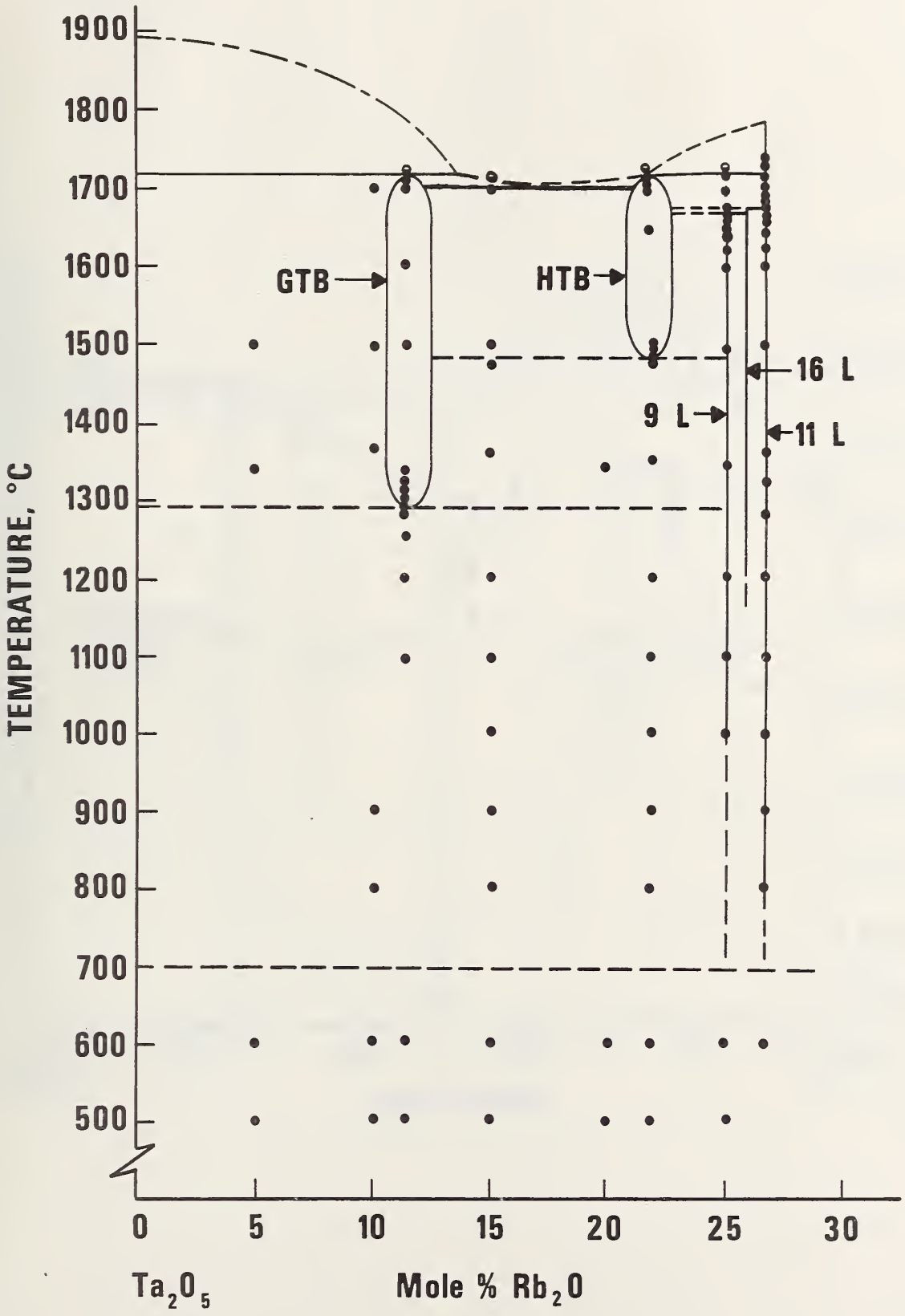
1900
1800
1700
1600
1500
1400
1300
1200
1100
1000
900
800
700
600
500
TEMPERATURE, °C
GTB
HTB
16 L
9 L
11 L
0
5
10
15
20
25
30
Ta_2O_5
Mole % Rb_2O

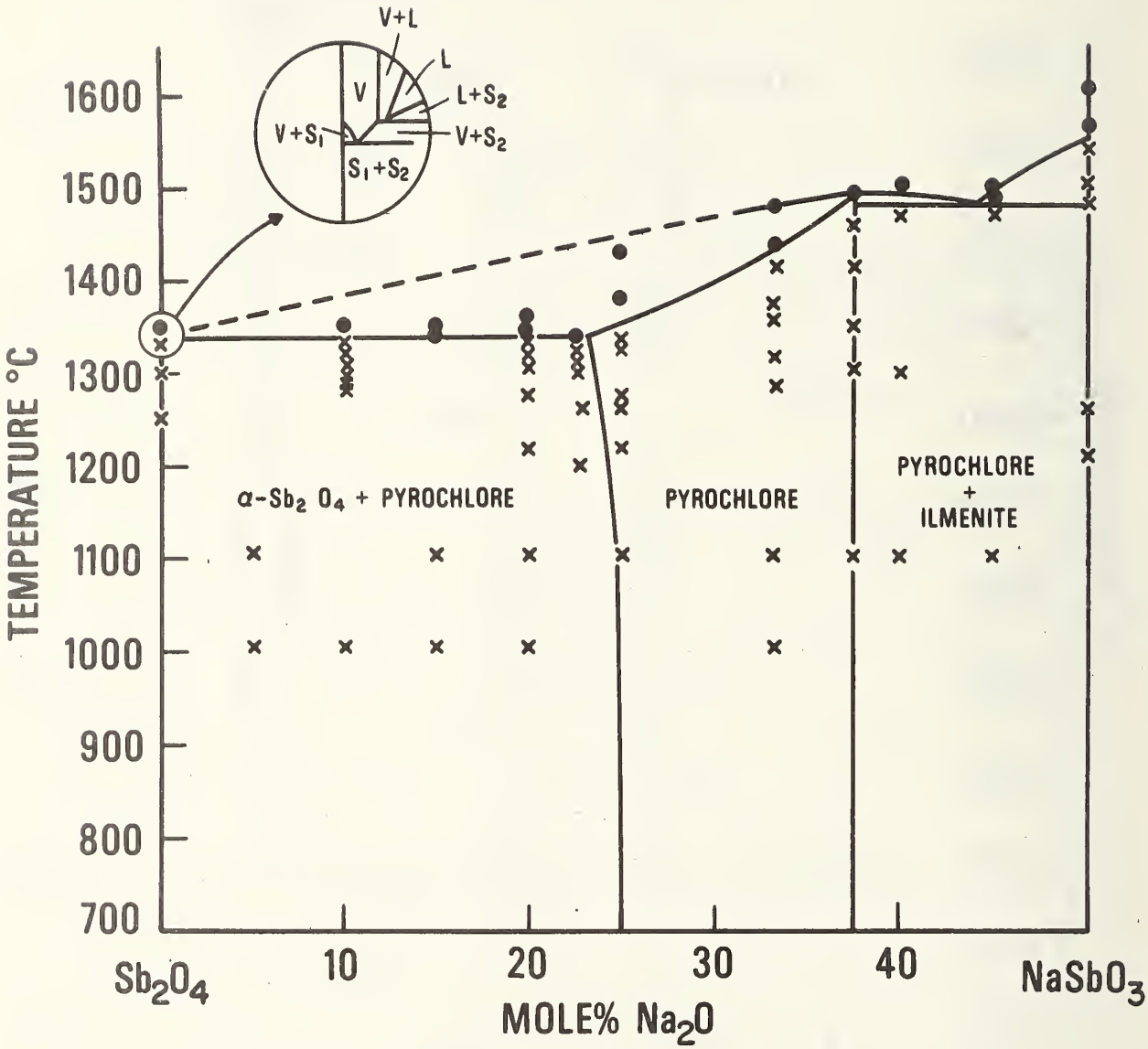
V+L
L
V
L+S2
V+S1
V+S2
S1+S2
1600
1500
1400
1300
1200
1100
1000
900
800
700
TEMPERATURE °C
α-Sb2 O4 + PYROCHLORE
PYROCHLORE
PYROCHLORE
+
ILMENITE
Sb2O4
10
20
30
40
NaSbO3
MOLE% Na2O

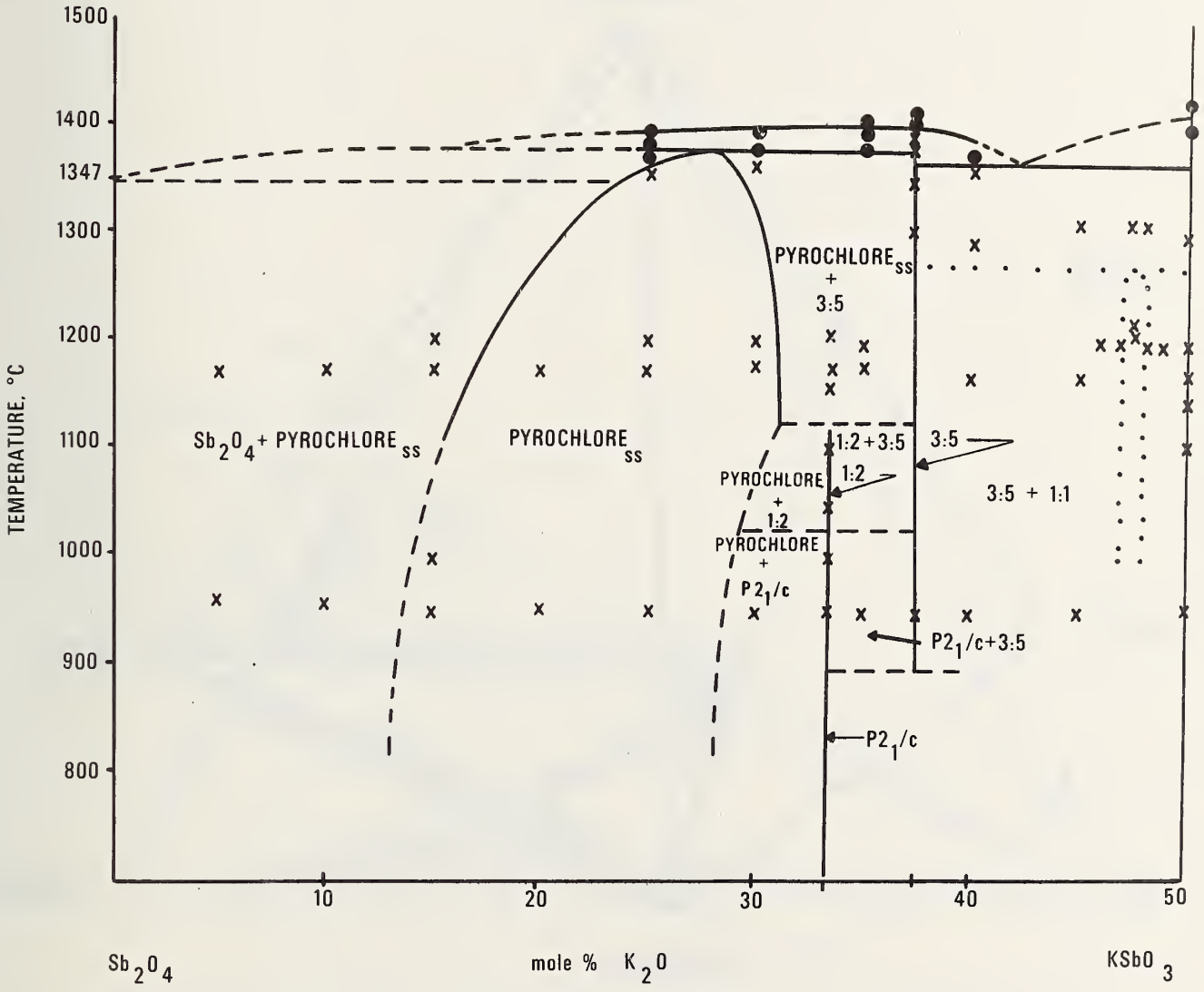
1500
1400
1347
1300
1200
1100
1000
900
800
TEMPERATURE, °C
PYROCHLORE$_{ss}$
+
3:5
Sb_2O_4 + PYROCHLORE$_{ss}$
PYROCHLORE$_{ss}$
1:2 + 3:5
3:5
PYROCHLORE
+
1:2
1:2
3:5 + 1:1
PYROCHLORE
+
$P2_1/c$
$P2_1/c$+3:5
$P2_1/c$
10
20
30
40
50
Sb_2O_4
mole % K_2O
$KSbO_3$

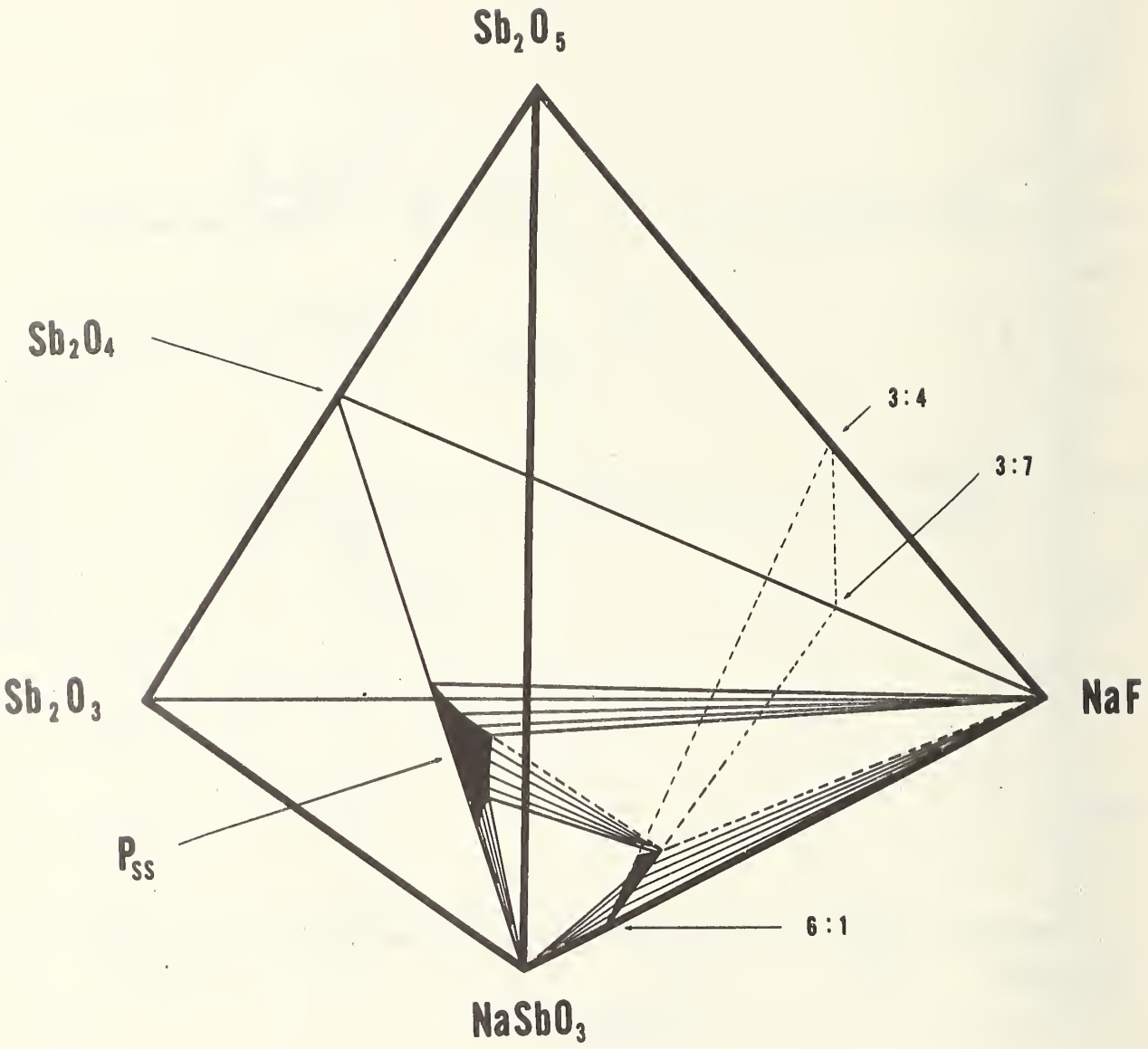
Sb_2O_5
Sb_2O_4
3:4
3:7
Sb_2O_3
NaF
P_{SS}
6:1
$NaSbO_3$

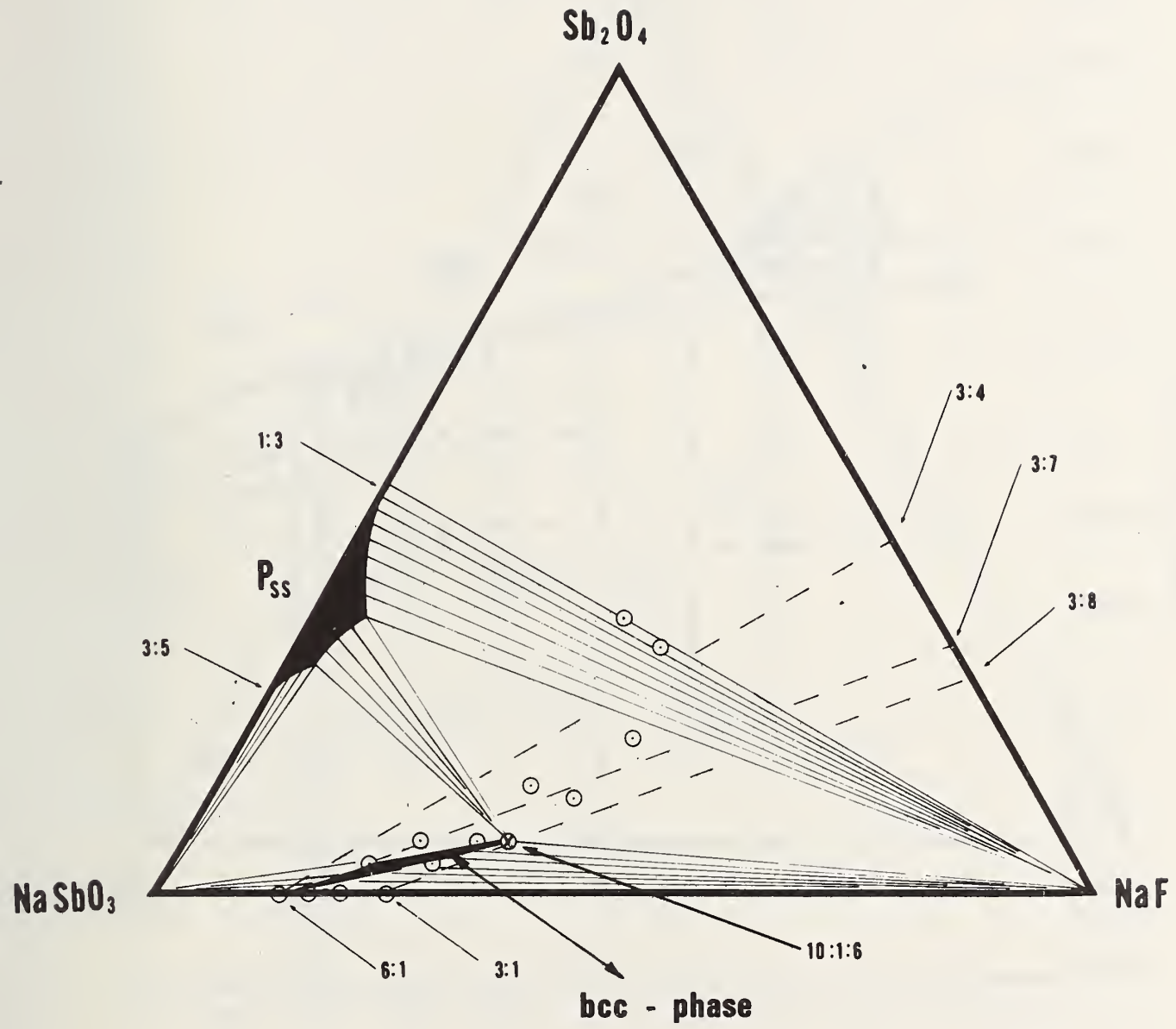
Sb_2O_4
1:3
3:4
3:7
3:8
3:5
P_{SS}
$NaSbO_3$
NaF
6:1
3:1
10:1:6
bcc - phase

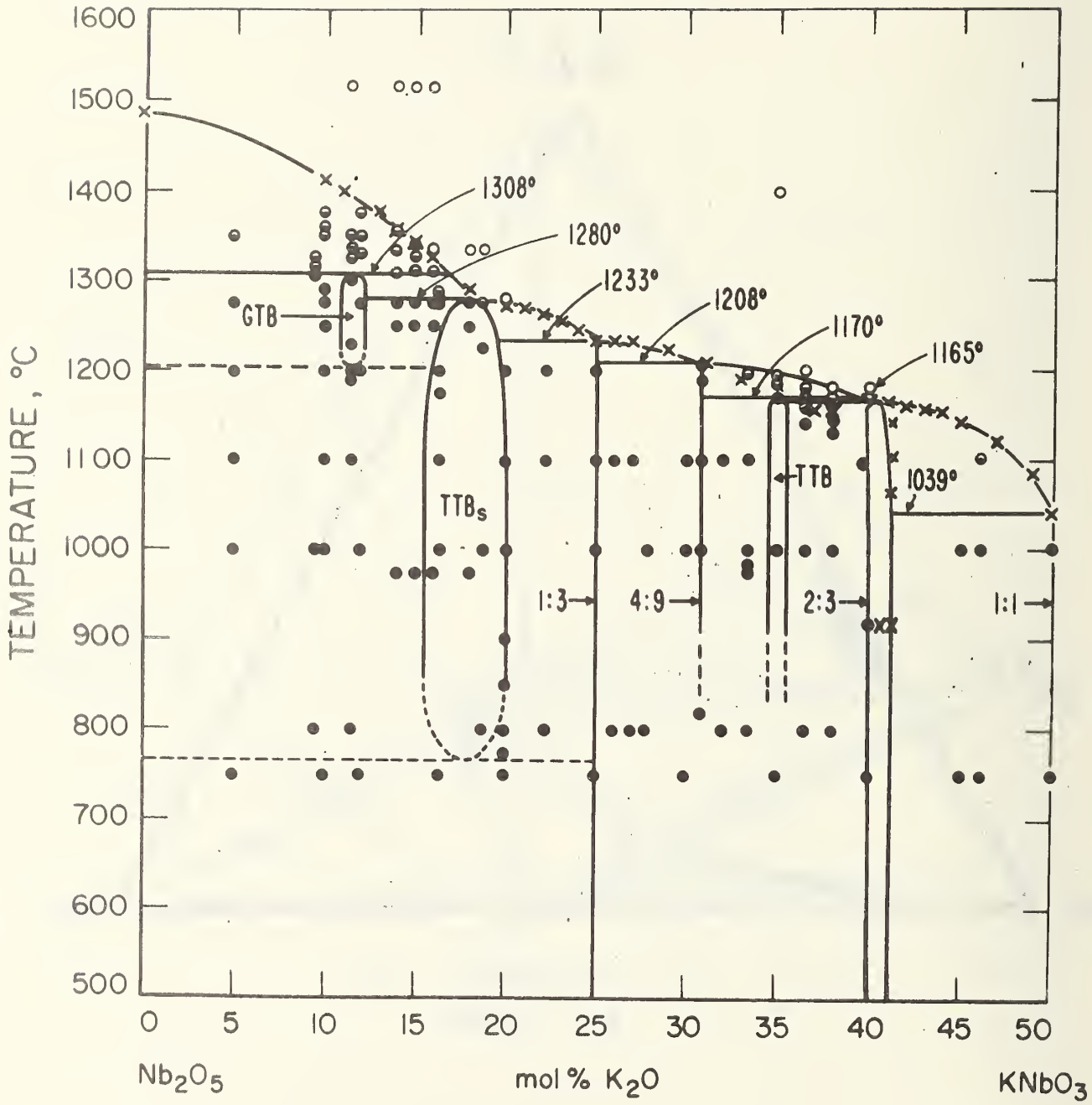
1600
1500
1400
1300
1200
1100
1000
900
800
700
600
500
TEMPERATURE, °C
1308°
1280°
1233°
1208°
1170°
1165°
1039°
GTB
TTBs
TTB
1:3
4:9
2:3
1:1
0
5
10
15
20
25
30
35
40
45
50
Nb2O5
mol % K2O
KNbO3

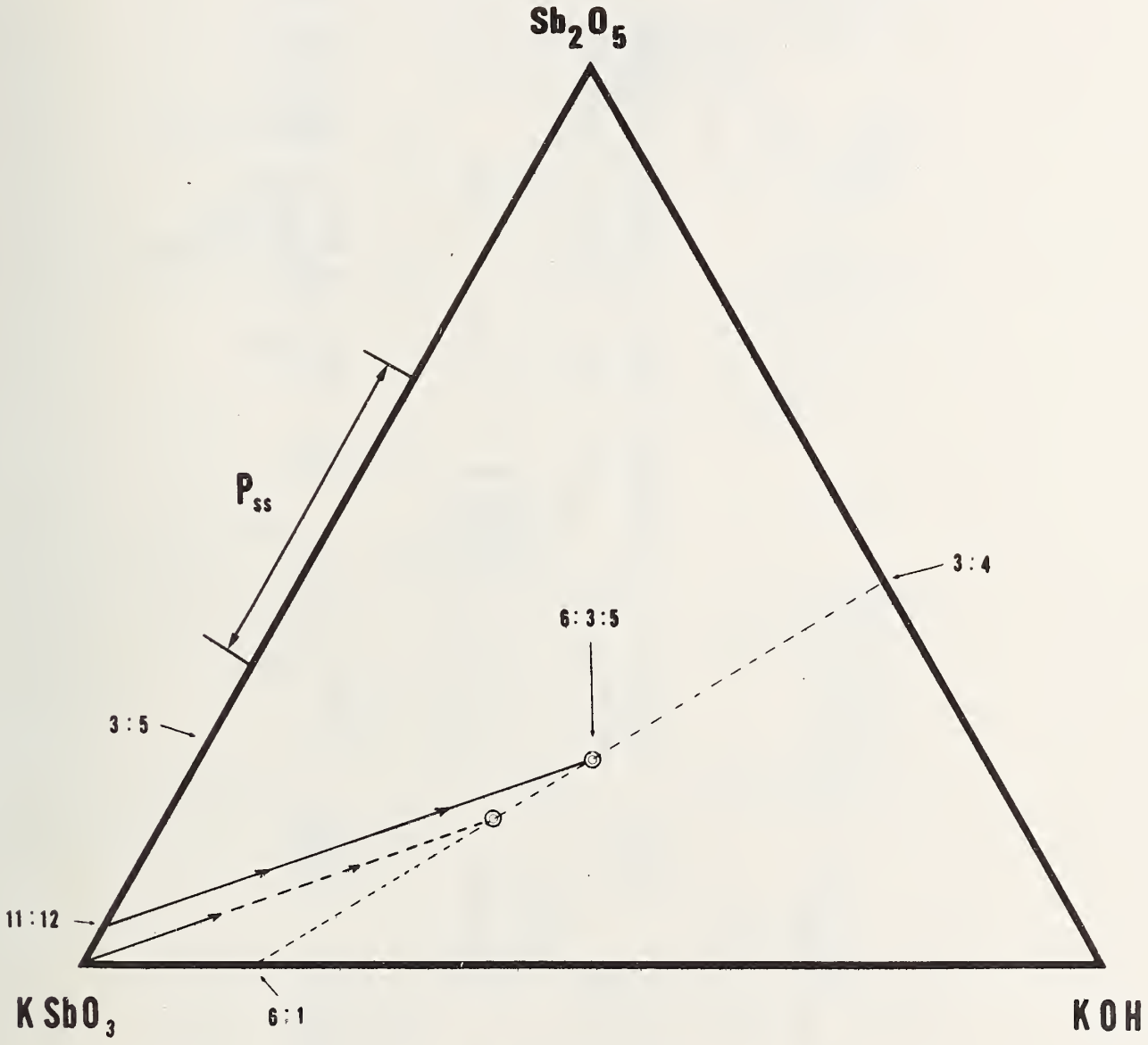
Sb_2O_5
P_{ss}
3 : 4
6 : 3 : 5
3 : 5
11 : 12
$KSbO_3$
6 : 1
KOH

Table 1. Experimental Data for the System Nb_2O_5-$4Rb_2O$:$11Nb_2O_5$.

Composition	Previous Heat Treatment Temp. °C	Previous Heat Treatment Time hr	Final Heat Treatment[a] Temp. °C	Final Heat Treatment[a] Time hr	Results of Physical Observation	Results of X-ray Diffraction Analysis
$5Rb_2O$:$95Nb_2O_5$			500	120[b]		H-Nb_2O_5 + 2:3
	500	120	600	90[b]		H-Nb_2O_5 + 3:17
	500	120				
	600	90				
			800	66		H-Nb_2O_5 + 3:17
			900	40		H-Nb_2O_5 + 3:17
			1000	80		H-Nb_2O_5 + 3:17
			1000	111[c]		
			1200	88		H-Nb_2O_5 + GTB
$10Rb_2O$:$90Nb_2O_5$			500	120[b]		H-Nb_2O_5 + 2:3
	500	120	600	90[b]		H-Nb_2O_5 + 2:3
	500	120				
	600	90				
			800	60		3:17 + H-Nb_2O_5
			900	40		3:17 + H-Nb_2O_5
			1000	80		3:17 + GTB + H-Nb_2O_5
			1000	111[c]		GTB + 3:17 + H-Nb_2O_5
			1075	60		GTB + H-Nb_2O_5
			1200	88		GTB + H-Nb_2O_5
$11.5Rb_2O$:$88.5Nb_2O_5$			500	120[b]		H-Nb_2O_5 + 2:3
	500	120	600	90[b]		H-Nb_2O_5 + 2:3
	500	120				
	600	90				
			800	60		3:17 + H-Nb_2O_5
			900	40		3:17 + H-Nb_2O_5
			1000	80		GT8 + 3:17
			1000	111[c]		GT8 + 3:17
	500	120				
	600	90				
	1000	111				
			1148	16		GT8
			1200	88		GT8
			1280	40		GTB
			1340	1.5	Not melted	
			1349	23		GT8
			1352	.25	Not melted	
			1355	.33	Not melted	
			1361	1	Not melted	
			1369	.5	Not melted	
			1375	1.5	Partial melted	GTB
			1380	2	Completed melted	
$15Rb_2O$:$85Nb_2O_5$			500	120[b]		H-Nb_2O_5 + 2:3
	500	120	600	90[b]		H-Nb_2O_5 + 2:3
	500	120				
	600	90				
			750	16[c]		11-L + H-Nb_2O_5
			750	16[d]		3:17
			800	66		3:17
			900	40		3:17
			1000	80		3:17
			1000	111[c]		3:17
			1075	60		3:17
			1200	88		GTB + HT8
	500	120				
	600	90				
	1000	111				
			1156	16.5		3:17
			1177	24		3:17 + GTB
			1180	23		3:17 + GT8
			1183	64		HT8 + GTB
			1226	18		HTB + GTB
			1262	18		--
			1349	23		HTB + GTB
	500	120				
	600	90				
	1000	111				
	1200	16.5				
			1153	84		GTB + 3:17
			1153	84[b]		CTB + 3:17
$20Rb_2O$:$80Nb_2O_5$			500	120[b]		H-Nb_2O_5 + 2:3
	500	120	600	90[b]		H-Nb_2O_5 + 2:3
	500	120				
	600	90				
			800	66		3:17 + 11-L
			900	40		3:17 + 11-L
			1000	80		3:17 + 11-L
			1000	111[c]		
			1200	88		9L + CT8 + HT8
$21.75Rb_2O$:$78.25Nb_2O_5$			500	120[b]		
	500	120	600	90[b]		
	500	120				
	600	90				
			800	66		3:17 + 11-L
			900	40		--
			1000	80		3:17 + 9-L + 11-L
			1000	111[c]		--
			1075	60		3:17 + 9-L
			1200	88		9-L + GTB
			1241	18		HTB + 9-L
			1250	16		HTB + 9-L
			1280	?		HTB + 9-L
			1300	16.5		HTB + 11-L + 16-L

	500	120				
	600	90				
	1000	111				
			1149	23		9-L + 3:17
			1169	18		9-L + 3:17
			1181	89		9-L + GTB
			1184	3.5		HTB + 9-L
			1313	64		HTB + 11-L
			1315	0.5	Not melted	
			1320	0.5	Partially melted	HTB + 11-L
			1320	22	Completely melted	HTB + 11-L
			1328	1.5	Completely melted	
			1347	16.5	Completely melted	
$23.19Rb_2O:76.81Nb_2O_5$						
	1000	63[c]				9-L + HTB
			1200	21[c]		9-L + HTB
			1255	18		9-L + HTB
			1290	18.5		9-L + HTB
			1306	22		HTB + 11-L
$25Rb_2O:75Nb_2O_5$			500	120[b]		Nb_2O_5 + 2:3
	500	120	600	90[b]		Nb_2O_5 + 2:3
	500	120				
	600	90				
			800	66		11-L + 3:17
			900	40		
			1000	80		11-L + 9-L
			1000	111[c]		
			1200	88		9-L
			1280	?		9-L + HTB
			1300	40		9-L
	500	120				
	600	90				
	1000	111				
			1290	18.5		--
			1300	16.5		11-L + HTB
$25.5Rb_2O:74.5Nb_2O_5$			500	63[b]		
	500	63	600	24[b]		
	500	63				
	600	24				
			1000	69[c]		9-L + 11-L
			1249	22		9-L
			1258	67		9-L + 16-L
			1262	16		9-L + 16-L
			1265	17		9-L + 16-L
			1275	117		16-L + ?tr
			1284	41		16-L + ?tr
			1285	18		16-L + 11-L
			1287	67		16-L + 11-L
			1291	21		16-L + 11-L
			1294	16		16-L + 11-L
			1297	22		16-L + 11-L
$26.67Rb_2O:73.33Nb_2O_5$			500	120[b]		H-Nb_2O_5 + 2:3
	500	120	600	90[b]		H-Nb_2O_5 + 2:3
	500	120				
	600	90				
			750	60		11-L
			800	66		11-L
			900	40		11-L
			1000	80		11-L
			1000	111[c]		11-L
			1075	60		11-L
			1200	88		11-L
			1241	18		11-L
			1280	40		11-L
			1300	40		H-L
	500	120				
	500	90				
	1000	111				
			1290	18.5		11-L
			1306	22		11-L
			1316	0.5	Not melted	
			1316	16	Partially melted	
			1320	0.5	Partially melted	
			1330	1.5	Completely melted	

[a] Except as indicated by a footnote the samples were quenched into water from the temperature indicated.

[b] The samples were calcined in open Pt crucibles and pulled from the furnaces at the temparatures indicated. Rb_2O may have been volatilized during these calcines thereby changing the composition to one greater in molé percent Nb_2O_5.

[c] The sample was a large sealed Pt tube and pulled from the furnace at the temperature and cooled rapidly on a chill block.

[d] The sample was removed from the furnace at the temperature indicated and immediately dunked into a beaker of water.

Table 2. Experimental Data for the System Ta_2O_5-$4Rb_2O$:$11Ta_2O_5$.

Composition	Initial Heat Treatment Temp. °C	Initial Heat Treatment Time hr	Final Heat Treatment[a] Temp. °C	Final Heat Treatment[a] Time hr	Results of Physical Observation	Results of X-ray Diffraction Analysis
$5Rb_2O:95Ta_2O_5$			500	120[b]		
	500	120	600	110[b]		$L\text{-}Ta_2O_5$
	500	120				--
	600	110				
			1340	120		$L\text{-}Ta_2O_5$ + GTB
			1500	144		$H\text{-}Ta_2O_5$ + GTB
$10Rb_2O:90Ta_2O_5$			500	120[b]		--
	500	120	600	110[b]		$L\text{-}Ta_2O_5$
	500	120				
	600	90				
			800	80		$L\text{-}Ta_2O_5$ + 9L
			900	60		$L\text{-}Ta_2O_5$ + 9L
			1366	120		GTB + $L\text{-}Ta_2O_5$
			1500	120		GTB + $H\text{-}Ta_2O_5$ (tr)
			1700	1		GTB
$11.5Rb_2O:88.5Ta_2O_5$			500	120[b]		--
	500	120	600	110[b]		--
	500	120				
	600	110				
			1098	136		$L\text{-}Ta_2O_5$ + 9L
			1255	27		9L + $L\text{-}Ta_2O_5$
			1318	16		9L + $L\text{-}Ta_2O_5$
			1340	120		GTB
			1500	144		GTB
			1603	24		GTB
	1200	150				
			1296	91		$L\text{-}Ta_2O_5$ + 9L + GTB (tr)
			1297	117		GTB + $L\text{-}Ta_2O_5$
			1307	64		GTB + $L\text{-}Ta_2O_5$
			1317	67		GTB + $L\text{-}Ta_2O_5$
			1327	18		GTB + $L\text{-}Ta_2O_5$
			1330	115		GTB + $L\text{-}Ta_2O_5$
			1332	16		GTB + $L\text{-}Ta_2O_5$
			1340	72		GTB
			1704	0.5	not melted	
			1709	0.5	not melted	
			1714	.25	not melted	
			1721	2	partially melted	GTB
			1722	1	completely melted	
	1330	115				
			1317	67		GTB
	1340	72				
			1277	136		GTB
			1297	117		GTB
	1277	136				
			1331	115		GTB
$15Rb_2O:85Ta_2O_5$			500	120[b]		
	500	120	600	110[b]		
	500	120				
	600	110				
			800	80		$L\text{-}Ta_2O_5$ + 9L
			900	60		$L\text{-}Ta_2O_5$ + 9L
			1000	40		$L\text{-}Ta_2O_5$ + 9L
			1098	136		$L\text{-}Ta_2O_5$ + 9L
			1360	120		GTB + 9L
			1473	65		GTB + 9L
			1500	17.5		GTB + HTB
			1500	18		GTB + HTB
			1500	144		GTB + HTB
			1700	2		GTB + HTB
	1200	150				
			1707	0.5	not melted	
			1711	0.5	not melted	
			1714	0.5	completely melted	
			1715	0.5	completely melted	
$20Rb_2O:80Ta_2O_5$			500	120[b]		
	500	120	600	110[b]		
	500	120				
	600	110				
			1340	120		9L + GTB

$21.75Rb_2O:78.25Ta_2O_5$			500	120[b]		
	500	120	600	110[b]		
	500	120				
	600	110				
			800	80		9L + L-Ta_2O_5
			900	60		9L + L-Ta_2O_5
			1000	40		9L + L-Ta_2O_5
			1100	138		9L + L-Ta_2O_5
			1360	120		9L + GTB
			1473	65		9L + GTB
			1500	18		9L + GTB
			1643	24		HTB + 9L (tr)
			1700	2		HTB
			1700	1		HTB
			1706	1		HTB
	1200	150				
			1474	67		9L + GTB
			1477	23		9L + GTB
			1477	18		9L + GTB
			1479	17		9L + GTB
			1479	18		9L + GTB
			1480	17		9L + GTB
			1482	18		9L + HTB (?)
			1482	45		9L + GTB
			1484	20		9L + GTB
			1486	41		9L + GTB
			1488	16		9L + HTB
			1488	16		9L + HTB
			1498	21		9L + HTB
			1706	1	not melted	
			1716	1	not melted	HTB
			1717	0.5	partially melted	
			1721	2	partially melted	HTB
$25Rb_2O:75Ta_2O_5$			500	120[b]		L-Ta_2O_5
	500	120	600	110[b]		
	500	120				
	600	110				
			1000	40		9L + L-Ta_2O_5 (tr)
			1100	138		9L
			1344	120		9L
			1498	144		9L + ? (tr)
			1675	18		16L + HTB
			1700	1		16L + HTB
			1700	1		16L + HTB
			1715	1	not melted	
	1200	150				
			1600	20		9L
			1621	3		9L
			1624	17		9L
			1641	21		9L
			1659	19		9L
			1663	67		9L + HTB (tr)
			1677	29		9L + HTB + 16L
			1682	18		16L + HTB
			1722	16	partially melted	
			1725	16	partially melted	16L + HTB
$26.7Rb_2O:73.3Ta_2O_5$			500	120[b]		L-Ta_2O_5 + 2:3
	500	120	600	110[b]		
	500	120				
	600	110				
			800	80		11L + 2:3
			900	60		11L + 2:3
			1000	40		11L + 2:3
			1098	136		11L + 2:3
			1360	120		16L + 11L
			1500	120		16L + 11L
			1596	24		16L + 11L
			1625	16		16L + 11L
			1640	2		16L + 11L
			1647	1		16L + 11L
			1700	1		11L
			1710	1	not melted	
	1200	150				
			1283	72		16L + 11L
			1672	1		11L
			1719	1	not melted	
			1725	0.5		11L
			1726	16		11L

[a] Except as indicated by [b] the samples were quenched into water from the temperature indicated.

[b] The samples were heated at the temperatures indicated in open Pt crucibles. Due to the volatility of Rb_2O the bulk composition may have shifted to one higher in mole percent Ta_2O_5.

Table 3. Experimental Data for Compositions in the System Sodium Antimonate-Antimony Tetroxide.

Composition		Heat Treatment[a]		Results	
Na_2O mole%	Sb_2O_4 mole%	Temp °C	Time hr	Physical Observation	X-ray Diffraction Analysis[b]
50	50	1213		not melted	
		1264	3	" "	$NaSbO_3$
		1435	1	" "	"
		1484	1	" "	
		1502	.08	" "	
		1542	.08	" "	$NaSbO_3$ + unknown
		1569	.08	melted	
		1602	.08	"	
45	55	1000	48	not melted	
		1100	48	" "	$NaSbO_3$ + pyrochlore ss
		1473	.25	" "	
		1488	.08	partially melted	
		1495	.08	completely melted	
40	60	1102	20	not melted	pyrochlore ss + $NaSbO_3$
		1305	19	" "	" "
		1430	.08	" "	
		1470	.08	" "	
		1488	.08	" "	
		1495	.03	completely melted	
37.5	62.5 (3:5)	1100	48	not melted	Pyrochlore ss
		1192	1	" "	
		1306	19	" "	pyrochlore ss
		1326	20	" "	
		1351	1	" "	
		1373	2	not melted (reheat of 1100-4)	pyrochlore ss
		1391	2	not melted	
		1392	.16	" "	pyrochlore ss
		1412	.16	" "	"
		1447	.16	" "	
		1454	.33	" "	
		1458	.08	" "	
		1464	.08	" "	
		1476	.08	" "	
		1487	.08	" "	
		1490	.08	melted	
33.33	66.67 (1:2)	1000[c]	8	not melted	
		1009[d]	168	" "	pyrochlore ss
		1100	3	" "	"
		1103[e]	91	" "	"
		1287	2	" "	"
		1292	1.5	" "	"
		1306	24	" "	
		1307	19	" "	pyrochlore ss
		1316	.5	" "	"
		1317	3.5	" "	
		1354	.75	" "	pyrochlore ss
		1360	24	" "	"
		1376	.5	" "	"
		1378	.5	" "	
		1411	19	" "	
		1418	.02	" "	
		1437	24	partially melted	
		1475	.02	completely melted	
25	75 (1:3)	750	60	not melted	pyrochlore ss + unknown[f]
		800	60	" "	pyrochlore ss + unknown[g]
		800	60	" "	pyrochlore ss + unknown[f]
		800	336	" "	pyrochlore ss + unknown
		1098	16	" "	pyrochlore ss
		1192	1	" "	"
		1200	24	" "	"
		1220	2	" "	"
		1277	2	" "	"
		1306	24	" "	
		1307	.08	" "	
		1317	16[h]	" "	pyrochlore ss
		1325	1	" "	
		1339	.08	" "	
		1345	.25	" "	pyrochlore ss
		1346	.08	" "	
		1358	.08	" "	
		1377	.02	partially melted	pyrochlore ss + $NaSbO_3$
		1427	.02	" "	
23	77	1200	24	not melted	pyrochlore ss + β-Sb_2O_4
		1266	4	" "	pyrochlore + α + β[i]/$_2$$O_4$
		1267	19	" "	pyrochlore ss[j]
		1299	.08	" "	
		1304	.08	" "	
		1313	.08	" "	
		1322	.08	" "	
		1332	.08	" "	pyrochlore ss[j]
		1338	.08	" "	

20	80	1099	672	not melted	pyrochlore ss[k]
		1107	144		
		1200	24	not melted	pyrochlore ss + α
		1220	2.5	" "	pyrochlore ss + α-Sb_2O_4
		1234	2.5	" "	" " "
		1277	16	" "	pyrochlore ss + β-Sb_2O_4
		1301	.5	not melted	---
		1305	19	" "	$NaSbO_3$[k]
		1306	24	" "	pyrochlore ss + β-Sb_2O_4
		1314	.08	" "	pyrochlore ss + α-Sb_2O_4
		1318	.08	" "	
		1335	.08	" "	
		1339	.2	" "	
		1340	.08	" "	
		1345	.2	partially melted	
		1362	.5	" "	
15	85	800	74	not melted	unknown + pyrochlore ss + α-Sb_2O_4[g,l]
		800	60	" "	α + pyrochlore ss + unknown[l]
		1000	64		unknown + tr α-Sb_2O_4 (dried 240)[g,l]
		1000	64		unknown + tr α-Sb_2O_4[g,l]
		1007	48	not melted	pyrochlore + α-Sb_2O_4 + unknown[l]
		1107	144	" "	pyrochlore ss + α-Sb_2O_4 + β-Sb_2O_4
		1200	24	" "	
		1200	60	" "	pyrochlore ss + α-Sb_2O_4
		1337	.2	" "	
		1340	.2	" "	
		1348	.2	partially melted	
10	90	800	74	not melted	α-Sb_2O_4 + unknown[l]
		1007	48	" "	α-Sb_2O_4 + β-Sb_2O_4 + pyrochlore ss[i]
		1107	144	" "	" " " "
		1234	2	" "	α-Sb_2O_4 + pyrochlore ss
		1281	.33	" "	" "
		1290	.33	" "	
		1300	.33	" "	α-Sb_2O_4 + pyrochlore ss
		1311	.2	" "	
		1319	.33	" "	
		1334	.33	" "	
		1337	.2	" "	α-Sb_2O_4 + pyrochlore ss
		1351	1	partially melted	α + pyrochlore ss + quenched liquid[m]
5	95	1007	48	not melted	β-Sb_2O_4 + α-Sb_2O_4 + pyrochlore ss[i]
		1107	144	" "	α-Sb_2O_4 + pyrochlore ss + trace β-Sb_2O_4[i]
		1234	3.5	" "	" " " " " "

[a] All specimens were preheated to 750°C for 60 hours and 1200°C for 19 hours unless otherwise footnoted. Rate of heating and cooling was approximately 3°/min. For higher heat treatments, speciments were heated in sealed Pt tubes and quenched from temperatures indicated.

[b] The phases identified are given in the order of the amount present (greatast amount first) at room temperature. These phases are not necessarily those present at the temperature to which the specimen was heated.

[c] Specimen heated with PtO_2 at 68,900 psi in sealed Pt tube.

[d] Specimen heated in sealed Pt tube at 5,000 psi.

[e] Specimen previously heated at 1292°C for 1.5 hours.

[f] Spacimen heated in sealed Pt tube in prasence of water. The unknown phase formed is probably a hydrate.

[g] Specimen heated in sealed Pt tube in PtO_2.

[h] Spacimen heated in presence of 5:95 Na_2O:Sb_2O_4 which served as a buffer.

[i] In spite of extensive x-ray study it has not been determined which of the polymorphic forms of Sb_2O_4 is the stable form.

[j] Sb_2O_4 probably soaked into Pt container and tha composition changed to pyrochlore ss.

[k] Platinum tube leaked.

[l] Unknown phase, d-spacing of major lines given in text. This phase is probably a hydrsted phase which exists in the presence of moisturs and/or PtO_2 and can be eliminated by an additional calcining of 1200°C for several hours. Once eliminated this phase does not appear to reform at lower temperatures in laboratory time.

[m] Specimen contained non-equilibrium material derived from a liquid when quenched from above the liquidus and examined at room temperature.

Table 4a. Experimental Data for Polymorphism in Antimony Tetroxide

Composition	Heat Treatment			Results	
Starting Material	Temp °C	Time hr	Environment	Physical Observation	X-ray Diffraction Analysis[a]
α-Sb_2O_4	1223	.5	sealed Pt tube	not melted	α + tr β
"	"	"	unsealed Pt tube	" "	α
β-Sb_2O_4	1223	.5	sealed Pt tube	not melted	β + tr α
"	"	"	unsealed Pt tube	volatilized	--
β-Sb_2O_4	1223	2	sealed Pt tube	not melted	β + tr α
α-Sb_2O_4	"	"	sealed Pt tube	" "	α + Sb_2O_3
α-Sb_2O_4	1303	19	sealed Pt tube	not melted	β + α
β-Sb_2O_4	"	"	" " "	" "	β
α-Sb_2O_4	1327	.08	sealed Pt tube	not melted	α + β
β-Sb_2O_4	"	"	" " "	" "	β + α
α-Sb_2O_4	1330	.25	sealed Pt tube	not melted	β + α
α-Sb_2O_4	1339	.08	sealed Pt tube	not melted	α + β
β-Sb_2O_4	"	"	" " "	" "	β + α
β-Sb_2O_4	1345	.08	sealed Pt tube	not melted	β + α
α-Sb_2O_4	1350	.08	sealed Pt tube	melted (vapor soaked into Pt)	--
β-Sb_2O_4	1350	.08	sealed Pt tube	melted ? large tabular vapor grown crystals	--
α-Sb_2O_4[b]	1200	-	high temperature x-ray		α (starting material remained α up to 1200°C)
α-Sb_2O_4[c]	750	24	open tray		α
"	800	"	" "		"
"	900	"	" "		α + β
"	950	"	" "		" "

[a] The phases identified are given in the order of the amount present (greatest amount first) at room temperature. These phases are not necessarily those present at the temperature to which the specimen was heated. α refers to α-Sb_2O_4 polymorph and β to the β-Sb_2O_4 polymorph.

[b] Material placed on platinum slide and heated and examined by x-ray diffraction at various temperatures.

[c] Poorly crystalline as received Sb_2O_4 was heated 750°C - 24 hours and the same specimen which was never ground was reheated at 800°C - 24 hours, then 900°C - 64 hours and finally 950°C - 24 hours.

Table 4b. Experimental High Pressure Data for Polymorphism in Antimony-Tetroxide.

Composition Starting Material	Heat Treatment Temp °C	Heat Treatment Time hrs	Environment	Pressure psi	Results[b] X-ray Diffraction Analysis
α-Sb_2O_4[a]	700	24	Sealed Au tube	88,000	β[c] + Sb_2O_3[d]
"	750	48	" " "	59,680	" " "
"	750	96	" " "	73,200	" " "
"	750	16	" " "	89,400	β + trace Sb_2O_3
"	751	116	" " "	109,000	β + Sb_2O_3
"	760	96	Sealed Au tube with PtO_2	80,000	β
"	766	96	Sealed Au tube	88,000	β + Sb_2O_3
"	775	115	" Pt "	47,500	α + Sb_2O_3
"	775	48	" Au "	54,760	β + Sb_2O_3
"	775	48	" Pt "	66,500	" " "
"	800	24	" Au "	93,000	" " "
"	800	24	Sealed Au tube with PtO_2	105,000	β
"	850	16	Sealed Au tube	82,500	β + Sb_2O_3
"	900	72	Sealed Pt tube with PtO_2	104,000	β
β-Sb_2O_4	900	72	" " " " "	104,000	β

[a] α-Sb_2O_4 prepared by the oxidation of Sb at 530°C on Pt tray. This material was reheated at 800°C - 60 hrs.

[b] The phases identified are given in the order of the amount present (greatest amount first) at room temperature. These phases are not necessarily those present at the temperatures to which the specimen was heated.

[c] β form of Sb_2O_4.

[d] High pressure form of Sb_2O_3 (valentinite).

Table 5. Experimental Data for Compositions in the System Potassium Antimonate-Antimony Tetroxide.

Composition		Heat Treatment[a]		Results	
K_2O Mole%	Sb_2O_4 Mole%	Temp °C	Time hr	Physical Observation	X-ray Diffraction Analysis[b]
5	95	950	60	not melted	pyrochlore ss + α-Sb_2O_4 + β-Sb_2O_4
		1168	48	" "	α-Sb_2O_4 + β-Sb_2O_4 + pyrochlore ss [c]
10	90	950	60	not melted	pyrochlore ss + α-Sb_2O_4 + β-Sb_2O_4 [c]
		1168	48	" "	" " "
15	85	853	24	not melted	
		950	60	" "	pyrochlore ss
		966	4	" "	
		1168	48	" "	pyrochlore ss + α-Sb_2O_4
		1200	19	" "	pyrochlore ss + α-Sb_2O_4 + β-Sb_2O_4
20	80	950	60	not melted	pyrochlore ss
		1168	48	" "	"
25	75	950	60	not melted	$P2_1/c$[d] + pyrochlore ss
		1179	48	" "	pyrochlore ss
		1361	.08	" "	
		1375	.08	partially melted	pyrochlore ss
		1385	.08	" "	
		1403	.08	completely melted	
30	70	950	60	not melted	$P2_1/c$[d] + pyrochlore ss
		1178	48	" "	1:2 + pyrochlore ss
		1366	.08	" "	
		1380	.08	partially melted	pyrochlore ss + 3:5
		1382	.08	" "	
		1399	.08	completely melted	
33.33	66.67	950	60	not melted	3:5 + $P2_1/c$[d]
		950	64	" "	
		998	70	" "	$P2_1/c$[d]
		1050	168	" "	
		1050[e]	168	" "	
		1102	1	" "	1:2[c] + 3:5 + pyrochlore ss + $P2_1/c$
		1106	64	" "	1:2[c] + 3:5 + pyrochlore
		1106[f]	64	" "	1:2 + 3:5
		1160[f]	1	" "	3:5 + pyrochlore ss
		1179	48	" "	1:2 + 3:5 + pyrochlore ss
		1214[f]	1	" "	3:5 + pyrochlore ss
		1214	2	" "	" "
35	65	950	60	not melted	pyrochlore + 3:5 + pyrochlore ss
		1178	48	" "	1:2 + 3:5
		1380	.08	partially melted	3:5 + pyrochlore
		1397	.08	" "	
		1409	.08	completely melted	
37.5	62.5	950	60	not melted	
		1174	88	" "	
		1195	19	" "	3:5
		1208	1	" "	3:5 + trace cubic
		950[e]	64	" "	
		1310	45	" "	3:5 + trace 1:1[g]
		1352	.08	" "	
		1379	.08	" "	
		1399	.08	completely melted	
		1416	.08	" "	
40	60	950	60	not melted	
		1174	88	" "	3:5 + cubic
		1208	1	" "	" "
		1295[e]	20	" "	3:5 + 1:1
		1362[e]	.5	" "	" "
		1375[e]	.08	partially melted	

45	55	950	60	not melted	1:1 + cubic + $P2_1/c$
		1174	88	" "	cubic + 3:5
		1208	1	" "	3:5 + cubic
		1311[e/]	1	" "	3:5 + 1:1
46	54	1200[h/]	1	not melted	cubic + 3:5
47	53	1194[h/]	3	not melted	cubic + trace 3:5
		1200	1	" "	cubic
47.5	52.5	1212[h/]	88	not melted	cubic + 3:5 + 1:1
		1218[h/]	17	" "	cubic + 1:1 + 3:5
		1310[g,h/]	45	" "	1:1
48	52	1198	3	not melted	cubic
		1200	1	" "	"
		1200[i/]	1.5	" "	cubic + 3:5 ilmenite
		1308	.5	" "	1:1
		1103[c/]	1	" "	cubic + ilmenite + pyrochlore
		1103[i/]	3	" "	ilmenite + pyrochlore
49	51	1200	1	not melted	cubic
50	50	750	70	not melted	
		800	24	" "	
		921	1	" "	
		946	21	" "	ilmenite
		950	60	" "	"
		1103	1	" "	"
		1104	22	" "	"
		1150	1	" "	"
		1174	88	" "	"
		1194	1	" "	"
		1202	1	" "	"
		1214	1	" "	"
		1298	.5	" "	"
		1363	.5	" "	"
		1403	.08	" "	"
		1421	.08	melted	
		1426	.08	" "	

[a/] All specimens were preheated to 500 and 700°C for 60 hours unless otherwise footnoted. Rate of heating and cooling were approximately 3°/min. Specimens were heated in sealed Pt tubes and quenched from temperatures indicated.

[b/] The phases identified are given in order of the amount present (greatest amount first) at room temperature. These phases are not necessarily those present at the temperature to which the specimen was heated. 1:2 - $K_2O \cdot 2Sb_2O_5$; 3:5 - $3K_2O \cdot 5Sb_2O_5$ and 1:1 - $KSbO_3$ - ilmenite structure.

[c/] Non-equilibrium mixture - see Discussion in text.

[d/] The phase was indexed from single crystal x-ray precession data which has shown the compound is monoclinic space group $P2_1/c$ a=7.178, b=13.378, c=11.985, β=124°10'.

[e/] This specimen was previously heated to 500°, 700° and 1200°C - 19 hours in a sealed Pt tube.

[f/] Specimen heated in open Pt tube.

[g/] Specimen leaked and changed composition.

[h/] Composition prepared from a mixture 1:1 and 3:5 - see text for explanation.

[i/] Specimen calcined and examined by x-ray diffraction while in form of pellet.

Table 6. Experimental Data for the Ternary System $NaSbO_3$-Sb_2O_4-NaF.

Composition	Mole %	Heat Treatment[a] Temp °C	Time hr	X-ray Analysis
$NaSbO_3$ Sb_2O_4 NaF	75.08 3.15 21.77	1250	19	single phase distorted cubic
$NaSbO_3$ Sb_2O_4 NaF	67.79 6.25 25.96	1250	19	body centered cubic + pyrochlore + ilmenite
$NaSbO_3$ Sb_2O_4 NaF	53.50 12.34 34.16	1250	19	body centered cubic + pyrochlore + sodium fluoride
$NaSbO_3$ Sb_2O_4 NaF	39.59 18.27 42.14	1250	19	body centered cubic + pyrochlore + sodium fluoride
$NaSbO_3$ Sb_2O_4 NaF	69.05 2.90 28.05	1250	19	body centered cubic + trace sodium fluoride
$NaSbO_3$ Sb_2O_4 NaF	49.28 11.37 39.35	1250	19	pyrochlore + body centered cubic + sodium fluoride
$NaSbO_3$ Sb_2O_4 NaF	31.20 28.87 39.93	1250	19	pyrochlore + sodium fluoride
$NaSbO_3$ Sb_2O_4 NaF	84.62 -- 15.38	1268	19	ilmenite + cubic
$NaSbO_3$ Sb_2O_4 NaF	74.42 2.32 23.26	1261 1268	1 19	distorted cubic + ilmenite distorted cubic + NaF
$NaSbO_3$ Sb_2O_4 NaF	70.00 3.33 26.67	1264	1	cubic + ilmenite
$NaSbO_3$ Sb_2O_4 NaF	65.96 4.26 29.78	1266 1267	1 19	cubic + ilmenite cubic + NaF
$NaSbO_3$ Sb_2O_4 NaF	62.96 4.94 32.10	1266 1267	1 19	cubic + NaF cubic + NaF
$NaSbO_3$ Sb_2O_4 NaF	58.82 5.89 35.29	1267	19	cubic + NaF
$NaSbO_3$ Sb_2O_4 NaF	68.00 4.00 28.00	1000 1252 1265 1265 1265	1 16 .1 1.5 72	ilmenite + trace NaF cubic + trace ilmenite cubic + NaF cubic + NaF cubic + NaF

[a] Preheated at 750°C for 60 hours open.

Table 7. Experimental Data for Alkali Bismuth Oxide Systems.

Composition	Temp. °C	Time hr	Results of X-ray Diffraction Analysis
$Na_2O:Bi_2O_3$	500	96	Bi_2O_3 + tr unknown
	500	120	Bi_2O_3
$K_2O:Bi_2O_3$	500	66	Bi_2O_3
	500	120	"
$K_2O:3Bi_2O_3$	500	66	Bi_2O_3

Table 8. Experimental Data for Alkali-Rare Earth Systems.

Composition	Temp °C	Time hr	Results of X-ray Diffraction Analysis
$Na_2O:Nd_2O_3$	800	23	α-Nd_2O_3
$K_2O:Nd_2O_3$	950	66	α-Nd_2O_3 + ?
$K_2O:3Nd_2O_3$	950	66	α-Nd_2O_3 + ?
$3K_2O:Y_2O_3$	600	20	Y_2O_3 + K_2CO_3
	700	20	" "
	800	20	" "
	950	66	Y_2O_3
$K_2O:Y_2O_3$	500	24	Y_2O_3
$Na_2O:Sm_2O_3$	800	23	Sm_2O_3
	950	1.5	
$Na_2O:3Sm_2O_3$	800	23	Sm_2O_3
	950	1.5	
$89.6Na_2O:10.4Sm_2O_3$	~1350	1[a]	Sm_2O_3
$K_2O:3Sm_2O_3$	800	23	Sm_2O_3
	950	1.5	
$K_2O:Sm_2O_3$	800	23	Sm_2O_3
	950	1.5	
	1250	16.5[b]	Sm_2O_3 + ?
	1350	17.5[b]	Sm_2O_3
$K_2O:Gd_2O_3$	750	90	--
	1000	92	--
	1365	67[b]	B-Gd_2O_3 + C-Gd_2O_3
	1370	16[b]	" "

[a] The sample was heated in an open Pt crucible in an induction heater and the temperature recorded via an optical pyrometer.

[b] Quenched from temperature indicated.

Table 9. Further Experimental Data for the System Nb_2O_5-$KNbO_3$.

Composition	Temp °C	Time hr	Results of X-ray Diffraction Analysis
$40.5K_2O:59.5Nb_2O_5$	600	40	
	750	84	
	1000	48	2:3 hydrate + TTB
	1000	48[a]	2:3 anhydrous + TTB
$41K_2O:59Nb_2O_5$	600	48	
	700	85	
	750	60	
	800	90	
	1000	48[a]	2:3 anhydrous
	1000	48	2:3 hydrate
	1000	48[c]	2:3 anhydrous
	1000	60[b]	" "

[a] Slide heated @ 220° for 96 hours.

[b] Slide heated > 125°C.

[c] Slide heated to 110°C.

Table 10a. Summary of Ion Exchange Experiments

EXCHANGE MEDIUM	TEMP °C	TIME	RESULTS
	$7K_2O:13Nb_2O_5$		
$NaNO_3$	340°	2 hr	Decomposed to $KNbO_3$ + KNb_3O_8 + H-Nb_2O_5
$3NaNO_2:2NaNO_3$	244°	24 hr	Unchengad 7:13(TTB)+Ne-TTB(?)
	244°	72 hr	Unchanged 7:13 + $NeNbO_3$(tr)
$NaNO_3$(aq)[a]	104°	2 hr	No chenga
	$18.75K_2O:81.25Nb_2O_5$		
$NaNO_3$	∿500°	2 hr	$NaNbO_3$
	330°	2 hr	H-Nb_2O_5 + residual TTB_s
	$11.5K_2O:88.5Nb_2O_5$		
$NaNO_3$(aq)[a]	100°	2 hr	Dacomposed to H-Nb_2O_5 + TTB_s
	$2K_2O:3Nb_2O_5$		
$NaNO_3$	∿500°	2 hr	$NaNbO_3$ perovskite
	340°	1 hr	Decomposed to KNb_3O_8 + $KNbO_3$
$NaNO_3$(aq)[a]	100°	2 hr	Decomposad to $NeNbO_3$
	25°	72 hr	higher hydrate (b=42.2) + TTB[d]
	25°	4 hr	higher hydrate (b=42.2) + TTB[d]
NeOH(aq)[b]	25°	18 hr	higher hydreta + TTB[d]
H_2O (deionized)	25°	18 hr	No chenge
NaI (ac)[c]	25°	18 hr	Unchanged 2:3 + TTB + higher hydrate (acatonata?)[d]
	$41K_2O:59Nb_2O_5$		
--	As prepared	hydrated	Hydrated "2:3"
--	As preparad	enhydrous	Singla pheae "2:3"
$NaNO_3$	450	3.5	Complete exchange
	500	1	Complata exchanga
	450	4	Palleta hydrated end decrepitated while baing x-rayed
	$KTeWO_6$		
$NaNO_3$	∿500°	2 hr	$NeTaO_3$
	315°	2 hr	two phases: $KTeWO_6$ + $NeTeWO_6$
$NaNO_3$(aq)[a]	105°	1 hr	$NaTaWO_6$ a=10.375
$RbNO_3$(aq)[a]	105°	1 hr	$RbTaWO_6$ (a=10.352) + unknown phase
H_2O (deionized)	100°	1 hr	$KTeWO_6$
	$K_{.3}Te_{.3}W_{.7}O_3$		
$NaNO_3$	∿500°	2 hr	$NaTaO_3$ + HTB
	340°	2 hr	No change
	$K_2O:2Te_2O_5$		
$NaNO_3$	∿500°	2 hr	No change using either 900° (rhomb) or 1300° (TTB) celcined starting matariel
	$4Rb_2O:11Nb_2O_5$[e]		
	Single Exchenge		
KNO_3	400°	3 hr	K exch. 11 L phase e=7.554 c=43.398
	400°	16 hr	K axch. 11 L phasa
KNO_3	400°	16 hr	K exch. 11 L phese
	450°	36	K axch. 11 L phese
$NaNO_3$	500	1 hr	Pertially exch. e=7.4 c=43.6
	450	64 hr	Pertially decomposed
	414	17 hr	Partially axch. a=7.458 c=43.19
	400	16 hr	Partielly axch. a=7.472 c=43.23

Double Exchange

KNO_3/400°/3 hr → $NaNO_3$/400°/1.5 hr	a=7.458	c=43.398
→ $NaNO_3$/400°/16 hr	a=7.368	c=43.869
KNO_3/400°/16 hr → $NaNO_3$/450°/66 hr	a=7.366	c=43.898
KNO_3/400°/16 hr → $NaNO_3$/450°/98 hr	a=7.332	c=43.997

$Rb_2O:3Nb_2O_5$

KNO_3	450°	3 hr	K exch. 9 L phase a=7.56 c=36.52

$21.75Rb_2O:78.25Nb_2O_5$ [e/]

Single Exchange

KNO_3	450°	18 hr	No exchange (?)
	450°	99 hr	
$NaNO_3$	450°	99 hr	Partial exchange, increase in 'c' and partial decomposition

Double Exchange

KNO_3/450°/18 hr → $NaNO_3$/450°/23 hr	Partial exchange

$RbTa_2O_5F$ (a=7.519 c=3.888)

Single Exchange

KNO_3	340°	2.5	Partial exch. (?) a=7.512 c=3.879
	340°	15	" "
	450°	16	" "
$NaNO_3$(aq. 20 w %)			No exchange
$NaNO_3$	340°	3.5	No exchange

Double Exchange

KNO_3/450°/16 hr → $NaNO_3$/340°/2 hr	No exchange
KNO_3/450°/16 hr → $NaNO_3$/450°/44.5 hr	Some decomposition + partial exchange a=7.51 c=3.814

$Rb_{1-5x}Nb_{3.4+x}O_9$

$NaNO_3$	∿500°	2 hr	Unchanged HTB + $Na_2Nb_4O_{11}$ (tr) + $NaNbO_3$ (tr)
	330°	2 hr	No change
$3NaNO_2:2NaNO_3$	240°	22 hr	No change
KNO_3	∿500°	2 hr	$KNbO_3$ + unchanged HTB

[a/] 20 percent by weight of nitrate in deionized water

[b/] 20 percent by weight of hydroxide in deionized water

[c/] 10 percent by weight salt in acetone

[d/] when dried at 220°C this "higher hydrate" or "acetonate" changes to a 2:3 type structure with a and c the same as original but with a very small b axis of 30.78A by comparison with the original b=33.019A.

[e/] single crystal fragments

Table 10b. Summary of Ion Exchange Experiments with $4Rb_2O:11Nb_2O_5$ Pellets.

Starting Material	Pressing History	Firing History	K^+ Exchange History	Na^+ Exchange History	Remarks
$4Rb_2O:11Nb_2O_5$ 500 °C-90 hr c/	10000 psi a/ 20000 psi b/	1200 °-7 hr			Pellets cracked during firing a = 7.522 c = 43.180
			KNO_3-20hr @ 400° partial exchange e/		Pellet fragment disintegrated a = 7.128, c = 43.469
		↑ 15°/hr 1200 °-7 hr	KNO_3 -16 hr @ 400° partial exchange	$NaNO_3$-18 hr @400°C partial exchange	Pellet fragment did not disintegrate K^+ a = 7.575, c = 43.469 Na^+ a = 7.390, c = 43.663
		↑5°/minute 1200°-1hr ↓5°/minute	KNO_3-1 hr @400° complete exchange		pellet did not disintegrate K^+ a = 7.545, c = 43.332
		↑3°/minute 1200-1 hr ↓3° minute	KNO_3-19 hr @400° complete exchange		pellet displayed some spalling K^+ a = 7.555 c = 43.428
500-120 hr 600-90 hr d/	10000 psi a/	1100°C- 1 hr	KNO_3-16 hr @400° complete exchange	$NaNO_3$-21 hr @400°	K^+ a = 7.551, c = 43.401 Na^+ cells not calculated due to broadness of lines in diffraction
		1100°C-1.5 hr	KNO_3 16 hr @400° partial exchange	$NaNO_3$-41 hr @400° partial exchange	Na exchanged pellet decomposed K^+ a = 7.547, c = 43.428 Na^+ a = 7.404, c = 43.332
		1100°C-1 hr	KNO_3-72 hr @400° complete exchange	$NaNO_3$-32 hr @300° partial exchange	K^+ a = 7.557, c = 43.442 Na^+ a = 7.484, c = 43.482
	10000 psi a/ 20000 psi b/	1100-1hr 1200-1 hr 1100 - 16 hr 1200 -2 hr	KNO_3- 16 hr @400 ° complete exchange		Pellet cracked during final 1200 ° firing K^+ a = 7.557 c = 43.442
500-90		↑5°/minute 1200-5 hr ↓5° minute	KNO_3-2 hr 400°C complete exchange		powder fired in open tube K^+ a = 7.549, c = 43.387
			KNO_3-18hr d/ @400° complete exchange	$NaNO_3$=18 hr @400° complete exchange	K^+ a = 7.553 c = 43.387 Na^+ a = 7.375 c = 43.830

a/= hydraulic pressure
b/= Isostatic pressure
c/= Without PVA binder
d/= with PVA binder
e/= Complete exchange

	a	b
RbNb =	7.522Å	43.180Å
KNb =	7.554Å	43.398Å
NaNb =	7.368Å	43.869Å

Table 11. Alkali Fluoride - Sb_2O_4: Flux Evaporation

Composition	Temp/Time	Results
$98KF:2Sb_2O_4$	1100°-1200°C 6 hrs	Solid + liquid x-ray shows $KSbO_{3-x}F_x$ small crystals formed
$88.0KF:7.2KSbO_3:4.8Sb_2O_4$	1100° - 1 hr	Solid + liquid small crystals formed
$90KF:2Sb_2O_4:8B_2O_3$	1100° - 2 hr, slow cool to 1000°	Solid + liquid small crystals formed
$95RbF:5Sb_2O_4$	900° - 1000°C 1 hr	Solid + liquid small crystals formed

Table 12. Summary of X-ray Data.

System	Designation	Composition Alkali Oxide	Composition Metal Oxide	Symmetry	Unit Cell Dimensions a	b	c	β	Conditions Limiting Possible Reflections	Probable Space Group
		Mola%	Mole%		Å	Å	Å			
Rb_2O-Nb_2O_5	11-L	26.67	73.33	Hexagonal	7.522	-	43.18	-	hkℓ:-h+k+ℓ=3n	R3,R$\bar{3}$,R32,R3m,R$\bar{3}$m
	16-L	25.5	74.5	Hexagonal	7.514	-	65.12	-	hhℓ:ℓ=2n	P6$_3$mc,P$\bar{6}$2c,P6$_3$mmc
	9-L	25	75	Hexagonal	7.518	-	36.353	-	hhℓ:ℓ=2n	P6$_3$mc,P$\bar{6}$2c,P6$_3$mmc
	HTB	21.75	78.25	Orthorhombic	12.991	7.550	7.796	-	hk0:h+k=2n h0ℓ:ℓ=2n	Pmcn
	GTB	11.5	88.5	Tetragonal	27.484	-	3.9757	-	h00:h=2n	P42$_1$2,P$\bar{4}$2$_1$m
Rb_2O-Ta_2O_5	11-L	26.67	73.33	Hexagonal	7.506	-	43.19	-	hkℓ:-h+k+ℓ=3n	R3,R$\bar{3}$,R32,R3m,R$\bar{3}$m
	9-L	-	-	Hexagonal	7.508	-	36.41	-	hhℓ:ℓ=2n	P6$_3$mc,P$\bar{6}$2c,P6$_3$mmc
	HTB	21.75	78.25	Hexagonal	7.531	-	3.907	-	none	P6/mmm
	GTB	11.5	88.5	Tetragonal	27.573	-	3.9018	-	h00:h=2n	P42$_1$,2,P$\bar{4}$2$_1$m
K_2O-Sb_2O_4	pyrochlore ss	(variable)								
		15	85	Cubic	10.331	-	-	-	hkℓ:h+k,k+ℓ=2n	Fd3m
		30	70	Cubic	10.381	-	-	-	0kℓ:k+ℓ=4n	
	1:2	33.33	66.67	Monoclinic	19.473	7.452	7.198	94°54.4'	hkℓ:h+k=2n	C2/m (11)
	P2$_1$/c	33.33	66.67	Monoclinic	7.178	13.378	11.985	124°10'	hkℓ:no conditions h0ℓ:ℓ=2n 0k0:k=2n	P2$_1$/c
	3:5	37.5	62.5	Orthorhombic	24.274	7.157	7.334	-	hkℓ:no conditions 0kℓ:k=2n h0ℓ:h=2n hk0:no conditions 00ℓ:no conditions	Pbam (11)
Na_2O-Sb_2O_4	pyrochlora ss	(variable)								
		25	75	Cubic	10.289	-	-	-	hkℓ:h+k,k+ℓ=2n	Pd3m
		37.5	62.5	Cubic	10.286	-	-	-	0kℓ:k+ℓ=4n	

Distribution List

NASA
Washington, D.C. 20546
Attn: RPP/E.M. Cohn

NASA
Attn: G.M. Ault, M.S. 3-13
Lewis Research Center
21000 Brookpark Road
Cleveland, Ohio 44135

NASA
Attn: L. Rosenblum, M.S. 302-1
Lewis Research Center
21000 Brookpark Road
Cleveland, Ohio 44135

NASA
Attn: J. Singer, M.S. 302-1 (10)
Lewis Research Center
21000 Brookpark Road
Cleveland, Ohio 44135

NASA
Attn: J. Toma, M.S. 302-1
Lewis Research Center
21000 Brookpark Road
Cleveland, Ohio 44135

NASA
Attn: Technology Utilization
Office, M.S. 3-19
Lewis Research Center
21000 Brookpark Road
Cleveland, Ohio 44135

G.E. Research and Development Center
Physical Chemistry Laboratory
Attn: Walter Roth
P.O. Box 8
Schenectady, New York 12301

University of Connecticut
Chemistry Dept., U-60
Attn: A.F. Wells
Storrs, Connecticut 06268

AFML/LPL
Dr. Vincent L. Donlan
Wright Patterson AFB, Ohio 45433

Yardney Electric Corporation
Power Sources Division
3850 Olive Street
Denver, Colorado 80207

Yardney Electric Division
82 Mechanic Street
Pawcatuck, Connecticut 02891

Dr. Charles Levine
Dow Chemical U.S.A.
Walnut Creek Research Center
2800 Mitchell Drive
Walnut Creek, California 94598

Prof. Donald M. Smyth
Materials Research Center
Lehigh University
Bethlehem, Pennsylvania 18015

Prof. John W. Patterson
Dept. of Metallurgy
Iowa State University
Ames, Iowa 50010

Prof. Rustum Roy
Materials Science Dept.
Pennsylvania State Univ.
University Park, Pennsylvania 16802

Prof. John H. Kennedy
Univ. of Calif. at Santa Barbara
Santa Barbara, California 93106

Dr. Paul Jorgensen
Stanford Research Institute
Menlo Park, California 94025

Dr. L. Topper
Div. of Advanced Technology
Applications
National Science Foundation
Washington, D.C. 20550

Mr. L.R. Rothrock
Union Carbide Corp.
8888 Balboa Avenue
San Diego, California 92123

Dr. Robert A. Huggins
Dept. of Materials Science
and Engineering
Stanford University
Stanford, California 94305

Dr. M. Stanley Whittingham
Esso Research & Engineering Co.
Linden, New Jersey 07036

Dr. Neill T. Weber
Ford Motor Co. Research Lab.
Dearborn, Michigan 48121

Prof. James I. Mueller
Ceramic Engineering Div.
University of Washington
Seattle, Washington 98195

Dr. Douglas O. Raleigh
North American Rockwell
Science Center
Thousand Oaks, California 91360

Dr. R. H. Doremus
Rensselaer Polytechnic Institute
Materials Division
Troy, New York 12181

Dr. Elton J. Cairns
Electrochemistry Dept.
General Motors Research Lab.
12 Mile-Mound Roads
Warren, Michigan 48090

NASA-Lewis Research Center
Attn: L.W. Schopen 500-206
21000 Brookpark Road
Cleveland, Ohio 44135

NASA-Lewis Research Center
Attn: N.T. Musial, 500-113
21000 Brookpark Road
Cleveland, Ohio 44135

NASA Scientific and Technical
Information Facility (10)
Attn: Acquisitions Branch
P.O. Box 33
College Park, Maryland 20740

NASA-Lewis Research Center (2)
Attn: Library 60-3
21000 Brookpark Road
Cleveland, Ohio 44135

Dr. A. M. Greg Andrus, Code SCC
NASA
Washington, D.C. 20546

Mr. Gerald Halpert, Code 764
Goddard Space Flight Center
NASA
Greenbelt, Maryland 20771

Mr. Thomas Hennigan, Code 761
Goddard Space Flight Center
NASA
Greenbelt, Maryland 20771

Mr. Louis Wilson, Code 450
Goddard Space Flight Center
NASA
Greenbelt, Maryland 20771

Mr. Jack E. Zanks, MS 488
Langley Research Center
NASA
Hampton, Virginia 23365

Mr. Charles B. Graff, S&E-ASTR-EP
George C. Marshall Space Flt. Center
NASA
Huntsville, Alabama 35812

Mr. W.E. Rice, EP5
Manned Spacecraft Center
NASA
Houston, Texas 77058

Mr. Daniel Runkle, MS 198-220
Jet Propulsion Laboratory
4800 Oak Grove Drive
Pasadena, California 91103

Mr. Aiji A. Uchiyama, MS 198-220
Jet Propulsion Laboratory
4800 Oak Grove Drive
Pasadena, California 91103

Dr. R. Lutwack, MS 198-220
Jet Propulsion Laboratory
4800 Oak Grove Drive
Pasadena, California 91103

U.S. Army
Electro Technology Laboratory
Energy Conversion Research Div.
MERDC
Fort Belvoir, Va. 22060

Harry Diamond Laboratories
Room 300, Building 92
Conn. Ave. & Van Ness St., N.W.
Washington, D.C. 20438

U.S. Army Electronics Command
Attn: AMSEL-TL-P
Fort Monmouth, New Jersey 07703

Director, Power Program, Code 473
Office of Naval Research
Arlington, Virginia 22217

Mr. Harry W. Fox, Code 472
Office of Naval Research
Arlington, Virginia 22217

Arthur M. Diness, Code 471
Office of Coal Research
Arlington, Virginia 22217

Mr. S. Schuldiner, Code 6160
Naval Research Lab.
4555 Overlook Avenue, S.W.
Washington, D.C. 20360

Mr. J. H. Harrison, Code A731
Naval Ship R&D Laboratory
Annapolis, Maryland 21402

Commanding Officer
Naval Ammunition Depot
(305, Mr. D. G. Miley)
Crane, Indiana 47522

Chemical Laboratory, Code 134.1
Mare Island Naval Shipyard
Vallejo, California 94592

Mr. Phillip B. Cole, Code 232
Naval Ordnance Laboratory
Silver Spring, Maryland 20910

Mr. Albert Himy, 6157D
Naval Ship Engineering Center
Center Bldg., Prince Georges Center
Hyattsville, Maryland 20782

Mr. Robert E. Trumbule, STIC
4301 Suitland Road
Suitland, Maryland 20390

Mr. Bernard B. Rosenbaum, Code 03422
Naval Ship Systems Command
Washington, D.C. 20360

Mr. R. L. Kerr, POE-1
AF Aero Propulsion Laboratory
Wright-Patterson AFB, Ohio 45433

Mr. Edward Rasking, LCC, Wing F
AF Cambridge Research Lab.
L. G. Hanscom Field
Bedford, Massachusetts 01731

Mr. Frank H. Mollura, TSGD
Rome Air Development Center
Griffiss AFB, N.Y. 13440

HQ SAMSO (SMTAE/Lt. R. Ballard)
Los Angeles Air Force Station
Los Angeles, California 90045

Dr. Jesse C. Denton
National Science Foundation
1800 G Street, N.W.
Washington, D.C. 20550

Aerospace Corporation
Attn: Library Acquisition Group
P.O Box 95085
Los Angeles, California 90045

Dr. R. T. Foley
Chemistry Department
American University
Mass. & Nebraska Aves., N.W.
Washington, D.C. 20016

Dr. H. L. Recht
Atomics International Division
North American Aviation, Inc.
P. O. Box 309
Canoga Park, Calif. 91304

Mr. R. F. Fogle, GF 18
Autonetics Division, NAR
P. O. Box 4181
Anaheim, Calif. 92803

Dr. John McCallum
Battelle Momorial Institute
505 King Avenue
Columbus, Ohio 43201

Mr. W. W. Hough
Bellcomm, Inc.
955 L'Enfant Plaza, S.W.
Washington, D. C. 20024

Mr. D. O. Feder
Bell Telephone Lab., Inc.
Murray Hill, New Jersey 07974

Dr. Carl Berger
13401 Kootenay Drive
Santa Ana. California 92705

Mr. Sidney Gross
M.S. 84-79
The Boeing Company
P.O. Box 3999
Seattle, Washington 98124

Mr. M. E. Wilke, Chief Engineer
Burgess Division
Gould, Inc.
Freeport, Illinois 61032

Dr. Eugene Willihnganz
C & D Batteries
Division of ELTRA Corporation
3043 Walton Road
Plymouth Meeting, Pennsylvania 19462

Prof. T. P. Dirkse
Calvin College
3175 Burton Street, S.E.
Grand Rapids, Michigan 49506

Mr. F. Tepper
Catalyst Research Corporation
6101 Falls Road
Baltimore, Maryland 21209

Mr. C. E. Thomas
Chrysler Corporation
Space Division
P.O. Box 29200
New Orleans, Louisiana 70129

Dr. L. J. Minnich
G. & W. H. Corson, Inc.
Plymouth Meeting, Pennsylvania 19462

Mr. J. A. Keralla
Delco Remy Division
General Motors Corp.
2401 Columbus Ave.
Anderson, Indiana 46011

Mr. J. M. Williams
Experimental Station, Bldg. 304
Engineering Materials Lab.
E. I. duPont de Nemours & Co.
Wilmington, Delaware, 19898

Dr. A. Salkind
ESB, Inc. Research Center
19 West College Avenue
Yardley, Pennsylvania 19067

Mr. E. P. Broglio
Eagle-Picher Industries, Inc.
P.O. Box 47, Couples Dept.
Joplin, MO 64801

Mr. V. L. Best
Elpower Corporation
2117 South Anne Street
Santa Ana, California 92704

Dr. W. P. Cadogan
Emhart Corporation
Box 1620
Hartford, Connecticut 06102

Dr. H. G. Oswin
Energetics Science, Inc.
4461 Bronx Blvd.
New York, New York 10470

Mr. Martin Klein
Energy Research Corporation
15 Durant Avenue
Bethel, Connecticut 06801

Dr. Arthur Fleischer
466 South Center Street
Orange, New Jersey 07050

Dr. R. P. Hamlen
Research and Development Center
General Electric Company
P.O. Box 43, Bldg. 37
Schenectady, New York 12301

Mr. Kenneth Hanson
General Electric Company
Valley Forge Space Tech. Center
P.O. Box 8555
Philadelphia, Pennsylvania 19101

Mr. Aaron Kirpich
Space Systems, Room M2614
General Electric Co.
P.O. Box 8555
Philadelphia, Pennsylvania 19101

Mr. P. R. Voyentzie
Battery Products Section
General Electric Company
P.O. Box 114
Gainsville, Florida 32601

Mr. David F. Schmidt
General Electric Company
777 14th Street, N.W.
Washington, D.C. 20005

Dr. R. Goodman
Globe-Union, Inc.
P.O. Box 591
Milwaukee, Wisconsin 53201

Dr. J. E. Oxley
Gould Ionics, Inc.
P.O. Box 3140
St. Paul, Minnesota 55165

Grumman Aerospace Corporation
S. J. Gaston, Plant 35, Dept. 567
Bethpage, Long Island, N.Y. 11714

Battery and Power Sources Division
Gulton Industries
212 Durham Avenue
Metuchen, New Jersey 08840

Dr. P. L. Howard
Centreville, Maryland 21617

Dr. J. G. Goodenough
Lincoln Laboratory
Lexington, Mass 02173

Dr. M. E. Ellion, Manager
Propulsion & Power Systems Lab.
Bldg. 366, MS 524
Hughes Aircraft Co.
El Segundo, California 90245

Mr. R. Hamilton
Institute for Defense Analyses
400 Army-Navy Drive
Arlington, Virginia 22202

Mr. N. A. Matthews
International Nickel Company
1000-16th Street, N.W.
Washington, D.C. 20036

Dr. Richard E. Evans
Applied Physics Laboratory
Johns Hopkins Univ.
8621 Georgia Avenue
Silver Spring, Maryland 20910

Dr. A. Moos
Leesona Moos Laboratories
Lake Success Park, Community Drive
Great Neck, New York 11201

Dr. R. A. Wynveen, Pres.
Life Systems, Inc.
23715 Mercantile Road
Cleveland, Ohio 44122

Dr. James D. Birkett
Arthur D. Little, Inc.
Acorn Park
Cambridge, Massachusetts 02140

Mr. Robert E. Corbett
Dept. 62-25, Bldg. 151
Lockheed Aircraft Corporation
P.O. Box 504
Sunnyvale, California 94088

Dr. R. Briceland
Institute for Defense Analyses
400 Army-Navy Drive
Arlington, Virginia 22202

Mr. S. J. Angelovich
Chief Engineer
Mallory Battery Company
South Broadway
Tarrytown, New York 10591

Dr. Per Bro
P. R. Mallory & Co., Inc.
Library
Northwest Industrial Park
Burlington, Massachusetts 01801

P. R. Mallory & Co., Inc.
Library
P.O. Box 1115
Indianapolis, Indiana 46206

Messrs. William B. Collins and
M. S. Imamura
Martin-Marietta Corporation
P.O. Box 179
Denver, Colorado 80201

Mr. A. D. Tonelli, MS 17, Bldg. 22
A3-830
McDonnell Douglas Astronautics Co.
5301 Bolsa Avenue
Huntington Beach, California 92647

Dr. Robert C. Shair
Motorola, Inc.
8000 W. Sunrise Blvd.
Ft. Lauderdale, Florida 33313

Rocketdyne Division
North American Rockwell Corp.
Attn: Library
6633 Canoga Avenue
Canoga Park, California 91304

Mr. D. C. Briggs
WDL Division
Philco-Ford Corporation
3939 Fabian Way
Palo Alto, California 94303

Power Information Center
University City Science Institute
3401 Market Street, Room 2210
Philadelphia, Pennsylvania 19014

RAI Research Corporation
225 Marcus Blvd.
Hauppauge, L.I., New York 11787

Southwest Research Institute
Attn: Library
P.O. Drawer 28510
San Antonio, Texas 78228

Mr. Joseph M. Sherfey
5261 Nautilus Drive
Cape Coral, Florida 33904

Dr. W. R. Scott (M 2/2154)
TRW Systems, Inc.
One Space Park
Redondo Beach, California 90278

Dr. Herbert P. Silverman (R-1/2094)
TRW Systems, Inc.
One Space Park
Redondo Beach, Calif. 90278

TRW, Inc.
Attn: Librarian TIM 3417
23555 Euclid Avenue
Cleveland, Ohio 44117

Dr. Jose Giner
Tyco Labs., Inc.
Bear Hill-Hickory Drive
Waltham, Massachusetts 02154

Union Carbide Corp.
Development Lab. Library
P.O. Box 6056
Cleveland, Ohio 44101

Dr. Robert Powers
Consumer Products Div.
Union Carbide Corporation
P.O. Box 6116
Cleveland, Ohio 44101

Dr. C. C. Hein, Contract Admin.
Research and Develpment Center
Westinghouse Electric Corporation
Churchill Borough
Pittsburgh, Pennsylvania 15235

1. Report No.	2. Government Accession No.	3. Recipient's Catalog No.
CR-134869	NBSIR 75-754	

4. Title and Subtitle	5. Report Date
ALKALI OXIDE-TANTALUM, NIOBIUM AND ANTIMONY OXIDE IONIC CONDUCTORS	April 1975
	6. Performing Organization Code

7. Author(s)	8. Performing Organization Report No.
R.S. Roth, W.S. Brower, H.S. Parker, D.B. Minor and J.L. Waring	NBSIR 75-754
	10. Work Unit No.

9. Performing Organization Name and Address	11. Contract or Grant No.
National Bureau of Standards Department of Commerce Washington, D.C. 20234	C-50821-C
	13. Type of Report and Period Covered Final Report January 1, 1974-December 31,1974

12. Sponsoring Agency Name and Address	14. Sponsoring Agency Code
National Aeronautics and Space Administration Lewis Research Center 21000 Brookpark Road Cleveland, Ohio 44135	

15. Supplementary Notes

16. Abstract

The phase equilibrium relations of four systems were investigated in detail. These consisted of sodium and potassium antimonates with antimony oxide and tantalum and niobium oxide with rubidium oxide as far as the ratio $4Rb_2O:11B_2O_5$ (B=Nb, Ta). The ternary system $NaSbO_3$-Sb_2O_4-NaF was also investigated extensively to determine the actual composition of the body centered cubic sodium antimonate. In addition, various other binary and ternary oxide systems involving alkali oxides were examined in lesser detail. The phases synthesized were screened by ion exchange methods to determine mobility of the alkali ion within the niobium, tantalum or antimony oxide (fluoride) structural framework. Five structure types were found to be of sufficient interest to warrant further investigation. These structure types are (1) hexagonal tungsten bronze (HTB), (2) pyrochlore, (3) the hybrid HTB-pyrochlore hexagonal ordered phases, (4) body centered cubic antimonates and (5) $2K_2O:3Nb_2O_5$. Although all of these phases exhibit good ion exchange properties only the pyrochlore has so far been prepared with Na^+ ions as an equilibrium phase and as a low porosity ceramic. Unfortunately Sb^{+5} in the channel apparently interferes with ionic conductivity in this case, although relatively good ionic conductivity was found for the metastable Na^+ ion exchanged analogs of $RbTa_2O_5F$ and $KTaWO_6$ pyrochlore phases. Small crystals of the other phases can generally be prepared by flux techniques and ion exchanged with Na^+. However, in the one case where congruency allows large crystals to be pulled from the melt ($4Rb_2O:11Nb_2O_5$) ion exchange techniques up to ~450°C are not sufficient to accomplish complete replacement with Na^+ ions.

17. Key Words (Suggested by Author(s))	18. Distribution Statement
Ionic conductivity; non-stoichiometry; potassium antimonate; rubidium niobate; rubidium tantalate; sodium antimonate; sodium antimonate fluoride	Unclassified - Unlimited

19. Security Classif. (of this report)	20. Security Classif. (of this page)	21. No. of Pages	22. Price*
Unclassified	Unclassified	76	$4.75

* For sale by the National Technical Information Service, Springfield, Virginia 22151.